

FerryBox

From On-line Oceanographic Observations to Environmental Information



Report Describing the Contribution of Ferrybox Data to Process Understanding in Different Dynamical Regimes

Contract number : EVK2-2002-00144

Deliverable number : D-5-1

Revision : 2.0

Co-ordinator:

Professor Dr. Franciscus Colijn

GKSS Research Centre
Institute for Coastal Research
Max-Planck-Strasse
D-21502 Geesthacht

<http://www.ferrybox.org>

Document Reference Sheet

This document has been elaborated and issued by the European FerryBox Consortium.

P 1		GKSS	GKSS Research Centre Institute for Coastal Research	Coordinator
P 2		NERC.NOC	NERC.NOC – National Oceanography Centre Southampton University and National Environment Res. Council formerly NERC.SOC – Southampton Oceanography Centre	
P 3		NIOZ	Royal Netherlands Institute of Sea Research	
P 4		FIMR	Finnish Institute of Marine Research	
P 5		HCMR (formerly NCMR)	Hellenic Centre for Marine Research (formerly National Centre for Marine Research)	
P 6		NERC.POL	Proudman Oceanographic Laboratory	
P 7		NIVA	Norwegian Institute for Water Research	
P 8		HYDROMOD	HYDROMOD Scientific Consulting	
P 9		CTG (formerly CIL)	Chelsea Technology Group (formerly Chelsea Instruments Ltd.)	
P 10		IEO	Spanish Institute of Oceanography	
P 11		EMI	Estonian Marine Institute (in cooperation with the Estonian Maritime Academy)	

This document is sole property of the European FerryBox Project Consortium.

It must be treated in compliance with its confidentiality classification.

Any unauthorised distribution and/or copying without written permission by the author(s) and/or the FerryBox Consortium in terms of the *FerryBox Consortium Agreement* and the relevant project contracts is strictly prohibited and shall be treated as a criminal act and as a violation of copyright and whatsoever applicable laws.

The responsibility of the content of this document is fully at the author(s).



The European FerryBox Project was co-funded by the European Commission under the Fifth Framework Programme of the European Commission 1998-2002 – Energy, Environment and Sustainable Development (EESD) Programme under contract no. EVK2-2002-00144





Document Control Table

Project acronym:	FerryBox	Contract no.:	EVK2-2002-00144		
Deliverable No.:	D-5-1	Revision:	2.0		
WP number and title:	FerryBox WP-5	Applications of FerryBox data			
Work Package Manager:	Roger Proctor – Proudman Oceanographic Laboratory				
Work Package Team:	FerryBox WP-5 Team				
Document title:	Report Describing the Contribution of Ferrybox Data to Process Understanding in Different Dynamical Regimes				
Document owner:	European FerryBox Project Consortium				
Document category:	Deliverable				
Document classification:	PU – Public				
Status:	Final				
Purpose of release:	Deliverable for the European Commission				
Contents of deliverable:	How Ferrybox data contribute to process understanding in different dynamical regimes.				
Pages (total):	38	Figures:	35	Tables:	1
Remarks:	Updated for publication on the FerryBox report CD and website.				
Main author / editor:	Roger Proctor	FerryBox WP-5 Leader	NERC.POL		
Contributors:	FerryBox WP-5 Team				
Main contacts:	FerryBox project coordinator:		Contact for this report:		
	Professor Dr. Franciscus Colijn GKSS Research Centre Institute for Coastal Research Max-Planck-Strasse D-21502 Geesthacht, Germany Tel.: +49 4152 87 – 1533 Fax.: +49 4152 87 – 2020 E-mail: franciscus.colijn@gkss.de		Dr. Roger Proctor POL, Proudman Oceanographic Laboratory 6 Brownlow Street UK- Liverpool L35DA, United Kingdom Tel.: +44 151 795 4856 Fax.: +44 151 795 4801 E-mail: rp@pol.ac.uk		
Project website:	http://www.ferrybox.org				





Table of Contents

Part I	Processes Observed by Ferrybox Measurements	5
I-1	Upwelling in the Gulf of Finland, Baltic Sea	5
I-2	The Origin of Low Salinity Intrusions in the Western English Channel.....	7
I-3	Linking an Intense Bloom of <i>Karenia Mikimotoi</i> in the Western English Channel to French Atlantic Rivers	9
I-4	Tidal Advection, Sediment Fluxes and Biological Processes in the Wadden Sea, Southern North Sea.....	10
I-5	Identifying Upwelling Events along the Spanish Coast of the Bay of Biscay.....	13
I-6	Impact of Tidal straining on Near Shore Salinity in Liverpool Bay	15
I-7	Characterising Eco-hydrodynamic Regimes and Fronts in the Irish Sea	17
I-8	Air-Sea Interaction Evidenced by Ferrybox Measurements in the Aegean Sea.....	20
	References for Part I	21
Part II	The Role of Numerical Models in Understanding Processes Observed by Ferrybox Measurements.....	22
II-1	Understanding the Role of Advection in Interpreting Ferrybox Data in the Southern North Sea	22
II-2	Understanding the Spatial Extent of Waters Sampled by Ferrybox Measurements in the Southern North Sea	26
II-3	The Irish Sea: Modelling the Long-term Variability of Temperature and Salinity in the Irish Sea: Implications for Ferrybox Measurements.....	29
	Acknowledgement	34
	References for Part II	34



List of Figures

Figure I-1:	Ferry route of the Tallink Ferry between Tallinn and Helsinki.....	5
Figure I-2:	Temperature deviations along the ferry line Tallinn-Helsinki showing upwelling events near the southern (28 May 2002) and northern (5 July 1999) coasts of the Gulf of Finland developing after 5 days of easterly or westerly winds, respectively.....	6
Figure I-3:	Route of the “Pride of Bilbao” ferry.....	7
Figure I-4:	Sea surface salinity between Portsmouth and Bilbao in 2003 showing low salinity waters entering the western English Channel (~48oN).....	8
Figure I-5:	Time series data of chlorophyll-fluorescence and salinity showing the coincidence in the timing of the bloom in <i>Karenia Mikimotoi</i> and the arrival of low salinity water in the western English Channel (49.1°N, 4.1°W).....	9
Figure I-6:	Ferry route Texel to Den Helder.....	10
Figure I-7:	Typical examples of the depth-averaged tidal and mean currents in the Marsdiep inlet.....	10
Figure I-8:	Cross-section averaged salinity and temperature in the Marsdiep tidal inlet for a period of 2 days.....	11
Figure I-9:	Daily averaged salinity (top) and daily standard deviation (bottom) in the Marsdiep tidal inlet for a period of one year.....	12
Figure I-10:	The monthly mean flux of suspended sediments through the Marsdiep tidal inlet.....	12
Figure I-11:	Measurements used in the study.....	13
Figure I-12:	A: SST annual cycle for 2004; B: FBPoB SST for spring/summer 2004 and wind fetch,.....	14
Figure I-13:	Time series of surface salinity (SSS) from IEOS6 (solid lines) and FBPoB (+).....	14
Figure I-14:	Birkenhead to Belfast ferry track.....	15
Figure I-15:	Surface salinity measured aboard the Ferry for days 0 – 160 in 2004 (top), Liverpool sea level maxima (middle), Mersey river flow (bottom).....	15
Figure I-16:	Mean temperature (blue), mean ± one standard deviation (red), maximum and minimum (green) for all crossings to Belfast the south of the Isle of Man between 15 December 2003 and 5 December 2005.....	17
Figure I-17:	Temperature gradients (°C km ⁻¹) from all the data on each route.....	18
Figure I-18:	Temperature gradients (°C km ⁻¹) along the ferry route south of the Isle of Man in summer (July, August, September) for 2004 (top) and 2005 (bottom).....	19
Figure I-19:	Sample ferry tracks, Athens to Heraklion across the Aegean Sea.....	20
Figure I-20:	Along-track space-series plots of surface temperature in the south Aegean Sea. Each trip lasts from the 21:00 hour (local time) to approximately 06:00 hour of the next day.....	20
Figure II-1:	Ferry track Cuxhaven – Harwich and position of the CEFAS Gabbard Buoy.....	22
Figure II-2:	Comparison between Salinity data from CEFAS Gabbard Buoy (upper panel) and Ferrybox data (lower panel) using from the nearest geographical point of the route to Gabbard station.....	23
Figure II-3:	Comparison of salinity data measured at CEFAS Gabbard Buoy (upper panel) with salinity data from passively tracers, observed with the Ferrybox and transported within the GCM (lower panel).....	24
Figure II-4:	Travel times for water parcels leaving the Gabbard Buoy.....	24
Figure II-5:	Chlorophyll fluorescence observed at CEFAS Gabbard buoy (upper panel) and chlorophyll fluorescence of water passively transported within the GCM (lower panel).....	25
Figure II-6:	Comparison between observed Ferrybox Chl Fluorescence (dots) and estimated chlorophyll for tracers starting from the CEFAS Gabbard Buoy and drifting to the ferry route (crosses).....	25



Figure II-7:	Model domain, bathymetry and ferry track Cuxhaven – Harwich.....	26
Figure II-8:	Simulated tracer distributions after different time steps (colour of particles depicts their depth). Left: release at spring low water Harwich, right: release at neap low water Harwich. (Black dot: release position W. Gabbard Buoy; dotted line: ferry track).....	27
Figure II-9:	Coverage with tracers released off Harwich along the ferry track at different times and collected over several days.	28
Figure II-10:	Characteristic salinity of a different tracer field.	28
Figure II-11:	Map showing model domain and standard Birkenhead to Belfast ferry route.	29
Figure II-12:	Comparison of predicted and observed near-surface temperatures at the Cypris station over the period 1960-1999.	32
Figure II-13:	Comparison of predicted and observed mean monthly, and mean annual near-bed salinities at the Cypris station over the period 1960 – 1999.	32
Figure II-14:	Temperature along ferry route: 1960-1999. Y-axis: model gridpoints.....	33
Figure II-15:	Salinity along ferry route: 1960-1999. Y-axis: model gridpoints.....	33

List of Tables

Table II-1:	Statistical comparison of observed temperatures and salinities and the corresponding predicted values for the simulated period, 1960 – 1999 (3397 CTD profiles). Results presented as mean error and root mean square (RMS) error.	31
-------------	---	----



Contribution of FERRYBOX Data to Process Understanding in Different Dynamical Regimes

Ferrybox data has the potential to inform on a wide range of processes. Here we provide examples of how the different ferries operated within the project contribute to process understanding. We are fortunate in that we have ferries operating in several different dynamical regimes, i.e.

- In the Baltic Sea, a brackish environment, semi ice-covered in winter, with low tidal energy
- In the Skagerrak, between the Baltic Sea and the North Sea, where the brackish Baltic Outflow dominates in a low tidal energy regime
- The southern North Sea, a tidally stirred sea affected by advection and coastal river plumes
- The English Channel, a tidally stirred sea
- The Irish Sea, a sea with 6 different shelf sea regimes crossed by the ferry
- The Bay Of Biscay / Biscay Shelf, open ocean water in the Atlantic Ocean and a run-off dominated shelf
- The Friesian Islands, strong tidally stirred shallow passage between islands
- The Aegean Sea, open ocean within the low tidal energy Mediterranean Sea

This report is in two sections.

In Part I a number of examples of processes observed by the Ferrybox measurements are reported. These are

- I-1 Upwelling in the Gulf of Finland, Baltic Sea
- I-2 The origin of low salinity intrusions in the western English Channel
- I-3 Linking an intense bloom of *Karenia Mikimotoi* in the western English Channel to French Atlantic rivers
- I-4 Tidal advection, sediment fluxes and biological processes in the Wadden Sea, Southern North Sea
- I-5 Identifying upwelling events along the Spanish coast of the Bay of Biscay
- I-6 Impact of tidal straining on near shore salinity in Liverpool Bay
- I-7 Characterising eco-hydrodynamic regimes and fronts in the Irish Sea
- I-8 Air-Sea interaction evidenced by Ferrybox measurements in the Aegean Sea.

In Part II we report 3 numerical model experiments designed to help elucidate Ferrybox measurements. These are

- II-1 Understanding the role of advection in interpreting Ferrybox data in the Southern North Sea
- II-2 Understanding the spatial extent of waters sampled by Ferrybox measurements in the Southern North Sea
- II-3 Modelling the Long-term Variability of Temperature and Salinity in the Irish Sea: implications for Ferrybox measurements.

Part I Processes Observed by Ferrybox Measurements

I-1 Upwelling in the Gulf of Finland, Baltic Sea

In the Gulf of Finland the seasonal thermocline is usually situated at the depth of 10-20 m. The phosphocline is located in the upper part of the thermocline and the nitracline is about 5 metres deeper (Laanemets et al., 2004). Thus, the upwelling events and wind induced mixing favour enrichment of the near-surface layer mainly with phosphate. According to the direct measurements during an upwelling event in 1999 a drop in surface layer temperature from 19 to 10 °C has been associated with an increase in phosphate concentration from 0.02 to 0.20 $\mu\text{mol l}^{-1}$ (Vahtera et al., 2005).

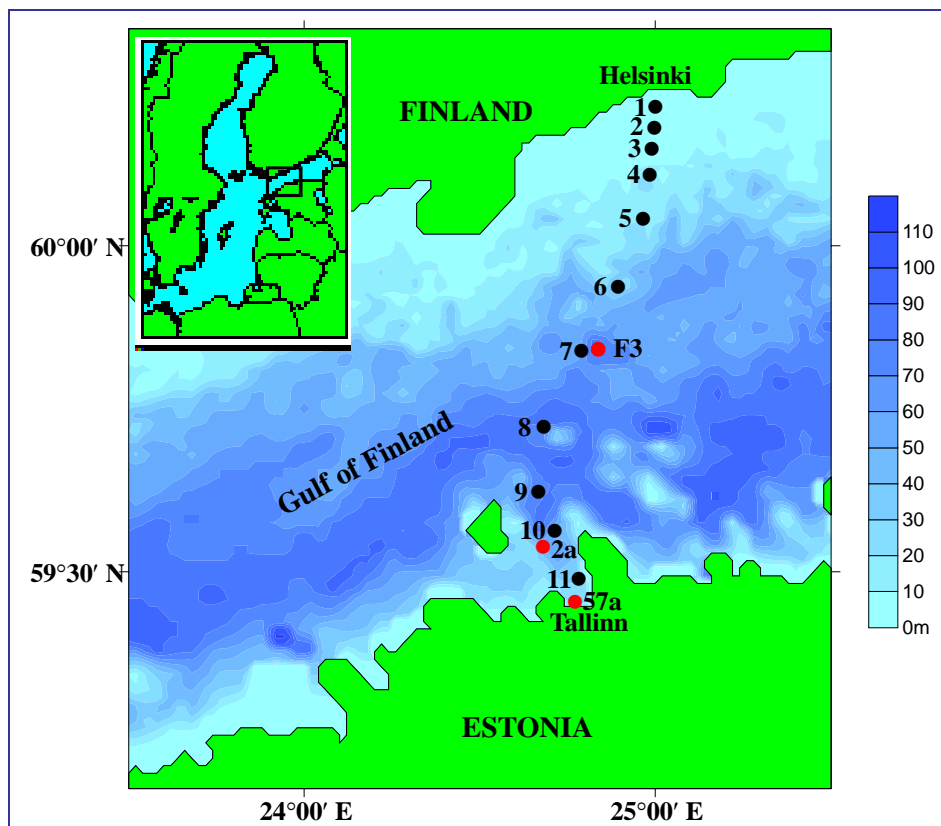


Figure I-1: Ferry route of the Tallink Ferry between Tallinn and Helsinki.

The twice a day Ferrybox measurements along the ferry line Tallinn-Helsinki (Figure I-1) can be used for identification and quantification of upwelling events. Successive temperature transects were analysed to describe initiation and development of upwelling events in relation to the wind characteristics. It is shown that upwelling events do not have the same dynamics because of the topographically different coasts of the gulf.

Cold upwelled water appears very close to the shoreline near the southern (Estonian) coast where the slope is steeper while it stays offshore from the Finnish coast (which is characterised by archipelagos). Figure I-2 illustrates the phenomena, occurring after a period of 5 days of steady winds, at the Estonian coast in response to easterly winds (28 May 2002) and at the Finnish coast in response to westerly winds (5 July 1999).

Since nutrient concentrations are not measured in a routine basis the nutrient input into the near-surface layer caused by the upwelling events could be estimated on the basis of unattended temperature measurements. One can make a rough assumption that the phosphate input from below the thermocline is proportional to the temperature difference between upwelled water and the surrounding water.

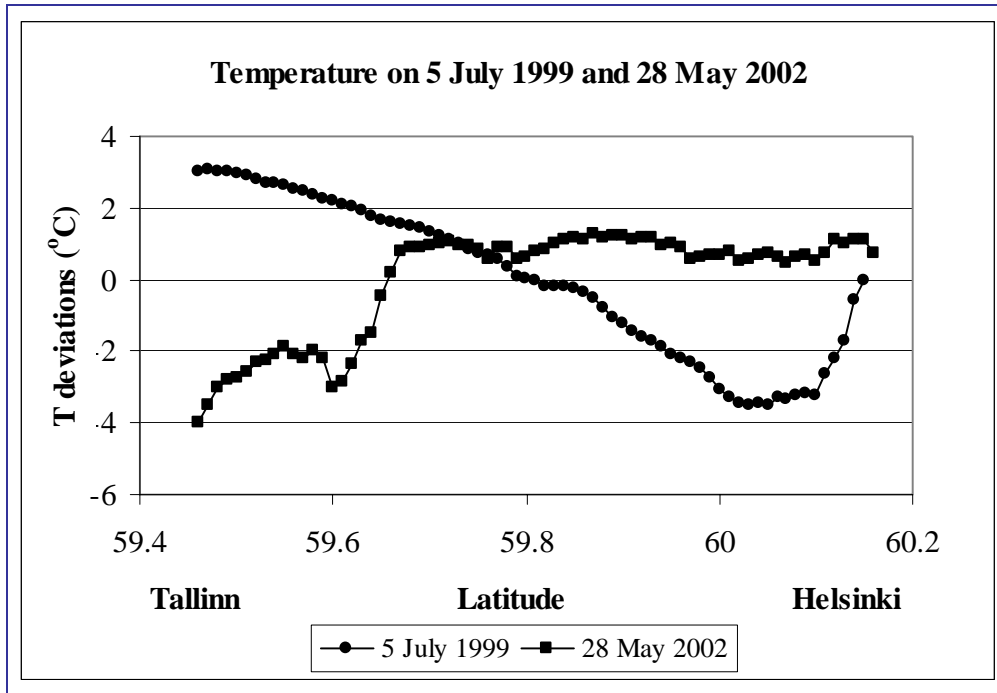


Figure I-2: Temperature deviations along the ferry line Tallinn-Helsinki showing upwelling events near the southern (28 May 2002) and northern (5 July 1999) coasts of the Gulf of Finland developing after 5 days of easterly or westerly winds, respectively.

An upwelling index is introduced and calculated as a mean temperature deviation in a 20-km wide coastal zone from the cross-gulf average temperature for every day. Operational estimates of intensities of pre-bloom upwelling events are used to forecast the late summer cyanobacterial blooms in the Gulf of Finland (Laanemets et al., 2006). Analysis of Ferrybox data from 1997-2004 revealed a good correlation between the seasonally integrated intensities of upwelling events (from 1 May until 30 June) and the integrated cyanobacterial bloom biomasses (Lips, 2005).

I-2 The Origin of Low Salinity Intrusions in the Western English Channel

During near continuous Ferrybox measurements from the ship of opportunity *Pride of Bilbao* sailing between Portsmouth and Bilbao (see Figure I-3) low salinity (<35) surface waters (LSSW) at the southern entrance to the western English Channel (48.5°N, 5.1°W, near Ushant) were observed in late winter (March – April) in three successive years (2002 – 2004).



Figure I-3: Route of the “Pride of Bilbao” ferry.

The LSSW intruded into the western English Channel in each year, suggesting a common phenomenon. The low salinity intrusion was freshest (mean = 35.11 ± 0.21) and most penetrative (reaching 50.7°N, 1.0°W by the end of the year) in 2003 (Figure I-4) on account of 1) entering on a spring tide giving greater tidal excursion into the western English Channel and 2) intrusion favourable winds (southwesterly/southeasterly) acting on the longer term residual flow.

Less penetration occurred in 2004 when the arrival of the LSSW coincided with a neap tide followed by intrusion-resistant northwesterly winds, resulting in a less saline (mean 35.20 ± 0.23) intrusion. In 2004 transport tended to be offshore to at least 100 km from the French Atlantic coast (47°N, 4.8°W - 48°N, 4.7°W). In 2002, the lower volume of plume water relative to the other years produced a more saline intrusion (mean = 35.25 ± 0.12). Prevailing westerly winds may have pushed this intrusion northwards beyond the route of the ferry, making it difficult to assess the true extent of the intrusion in 2002. A link of the LSSW to phases of the winter North Atlantic Oscillation index from a literature search of the last 84 years was inconclusive.

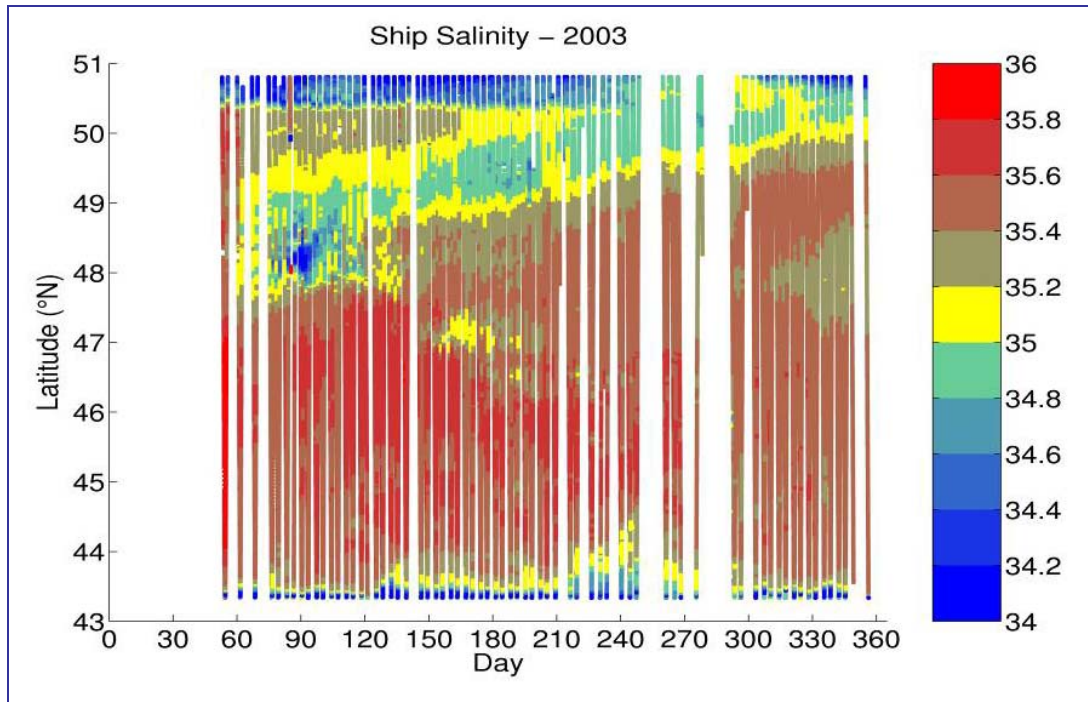


Figure I-4: Sea surface salinity between Portsmouth and Bilbao in 2003 showing low salinity waters entering the western English Channel (~48°N)

The source of the LSSW is the northward spreading plumes from the Loire (47.5°N, 2.5°W) and Gironde (45.6°N, 1.2°W) along the French Atlantic coast (Kelly-Gerreyn et al. 2006). Fastest plume travel times were associated with northeasterly winds, consistent with Ekman theory. Differences between years in the mean winter (January – March) combined river discharges (D) was consistent with the minimum salinities (S_{\min}) of the LSSW (2004: $D = 4211 \text{ m}^3 \text{ s}^{-1}$, $S_{\min} = 33.68$; 2003 : $D = 3630 \text{ m}^3 \text{ s}^{-1}$, $S_{\min} = 33.90$; 2002 : $D = 1579 \text{ m}^3 \text{ s}^{-1}$, $S_{\min} = 34.53$). Winter mean (1905 – 1974) salinity is otherwise 35.33 near Ushant.

I-3 Linking an Intense Bloom of *Karenia Mikimotoi* in the Western English Channel to French Atlantic Rivers

An intense monospecific bloom ($\sim 100 \text{ mg Chl a m}^{-3}$) of the dinoflagellate *Karenia Mikimotoi* was observed with the “Pride of Bilbao” Ferrybox system in the western English Channel in summer 2003. This species regularly occurs in these waters but there is significant interannual variability in the intensity of the bloom. The onset of the bloom in 2003 occurred within 2 days of the arrival of low salinity (<35) waters (Figure I-4) originating from French Atlantic rivers (Loire and Gironde) as described above.

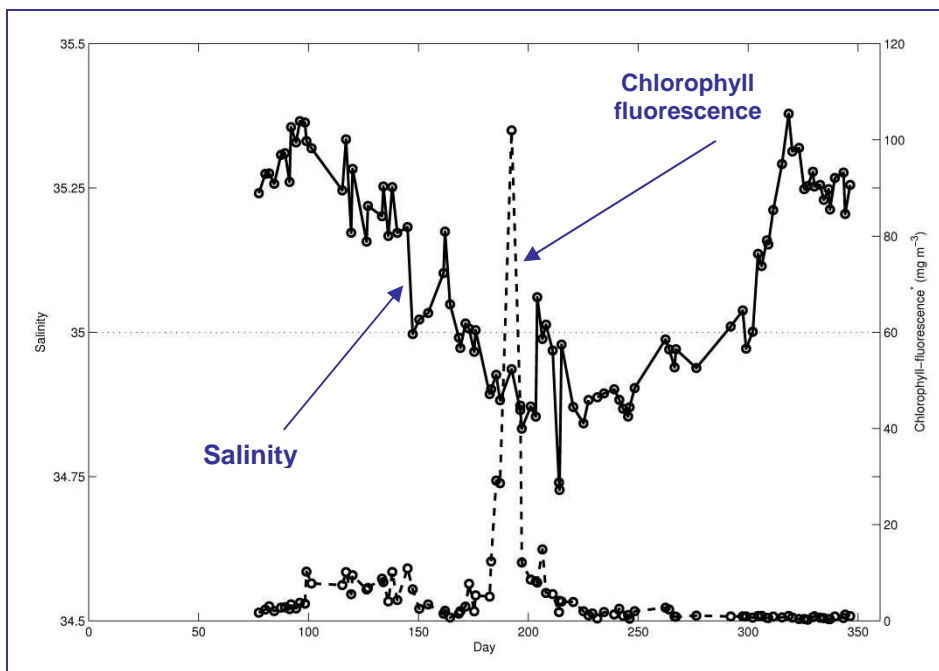


Figure I-5: Time series data of chlorophyll-fluorescence and salinity showing the coincidence in the timing of the bloom in *Karenia Mikimotoi* and the arrival of low salinity water in the western English Channel (49.1°N, 4.1°W).

It is proposed that changes in surface density due to these low salinity intrusions influences the summer bloom intensity of *Karenia Mikimotoi*. The hypothesis is that the low salinity intrusions enhance blooms of *Karenia Mikimotoi* through increased buoyancy of the upper water column and thereby influence the observed interannual variability in the abundance of this phytoplankter in the western English Channel.

I-4 Tidal Advection, Sediment Fluxes and Biological Processes in the Wadden Sea, Southern North Sea

The ferry from Texel to Den Helder across the Marsdiep tidal inlet (the northern coast of the Netherlands, Figure I-6) is equipped with a vessel-mounted acoustic Doppler current profiler (ADCP). The instrument is attached to the hull of the ferry at some 30 cm below the hull itself to prevent problems with air bubbles. The technical quality of the observations appears to be good.



Figure I-6: Ferry route Texel to Den Helder.

Tidal currents flow east/west through the inlet and reach maximum values of around 1.5 m/s, with strongest currents in the deepest central part of the inlet (Figure I-7). The strength of the tidal mean current is about 10% of the time-varying tidal currents and is asymmetric with large spatial variability over the relatively short distance of the inlet (about 4 km). At the northern site of the inlet the mean currents are westward (towards the adjacent North Sea), at the southern site the currents are eastward.

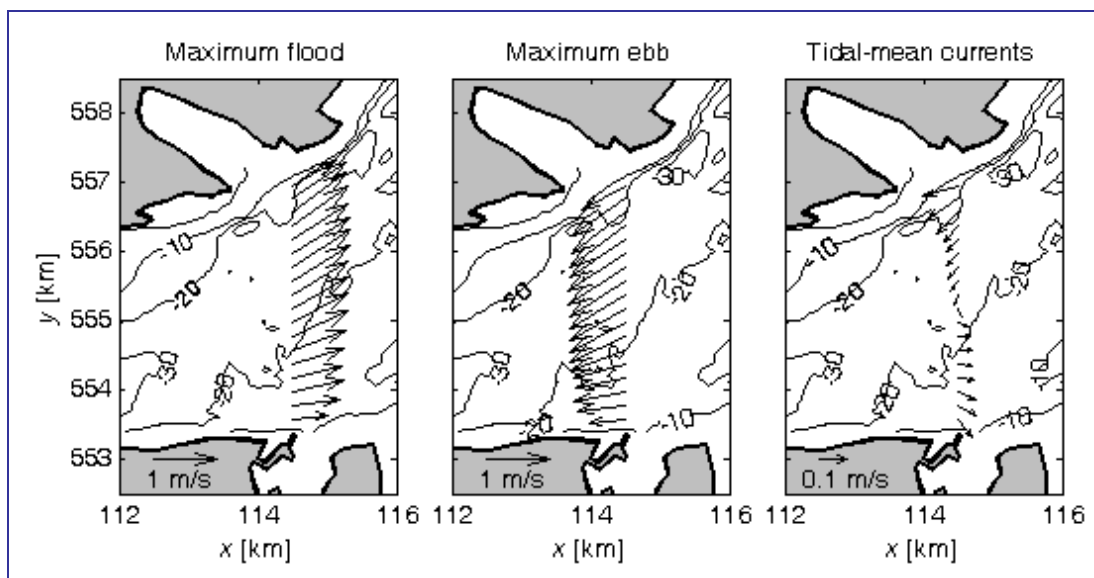


Figure I-7: Typical examples of the depth-averaged tidal and mean currents in the Marsdiep inlet.

The influence of wind or river inflow on these tidal mean currents appears to be relatively weak because they are mainly caused by the interaction between the tidal currents and the topography.

Temperature (T) and salinity (S) variations across this inlet are largely dominated by the tidal variations in the currents, e.g. the 2 days of observations shown in Figure I-8. The tidal influence on these observations is clear. Salinity increases (decreases) during flood (ebb) when saltier water from the adjacent North Sea enters the Wadden Sea through the tidal inlet. A similar variability is seen in the temperature variations. Both show that differences in T and S between the Wadden Sea and North Sea can be large and these data can be used to study (variations in) the hereby induced longitudinal density gradient across the tidal inlet.

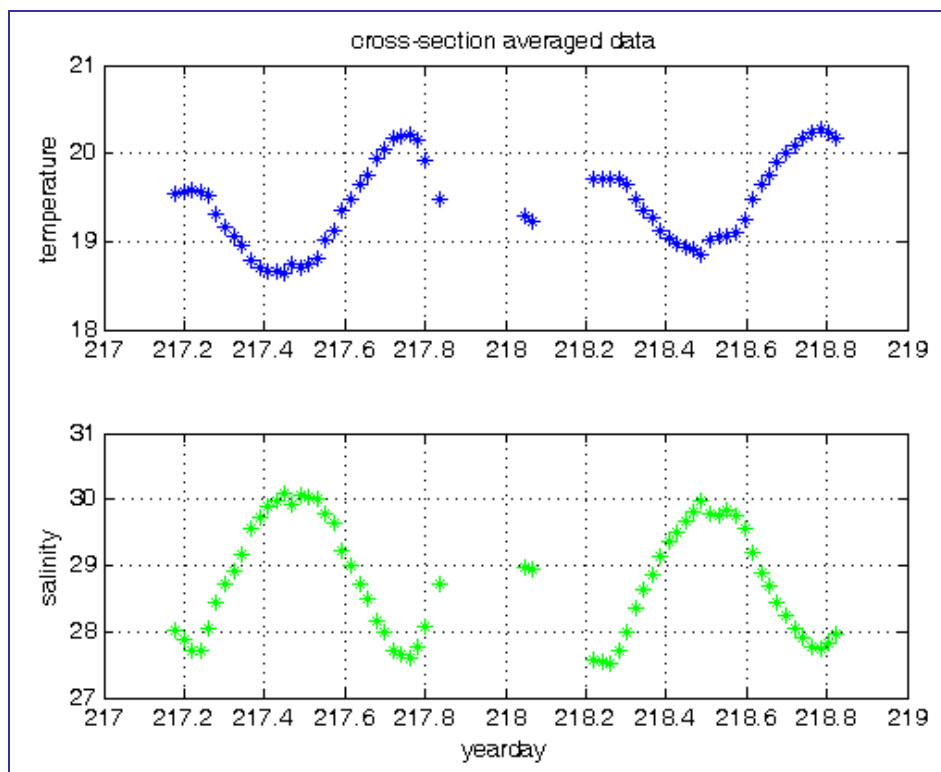


Figure I-8: Cross-section averaged salinity and temperature in the Marsdiep tidal inlet for a period of 2 days.

Longer term variability in the salinity observations is shown in Figure I-9 where daily averaged values (top) and the daily standard deviation (bottom) is shown for a typical year. Salinity values are lowest in winter and spring when the input of fresh water into the coastal zone from the rivers is largest. A relatively low mean salinity coincides with relatively high daily variability in salinity values. Thus, as expected, salinity differences between the North Sea and Wadden Sea are largest when the input of fresh water to the coastal zone (mostly from the Rhine and its associated overflows) is largest.

The observations of currents and backscatter from the ADCP are used to obtain insight in the current field and suspended sediment concentration (SSC) in the tidal inlet that forms the connection between the westernmost tidal basin of the Wadden Sea and the adjacent North Sea. The long duration and, especially, the high frequency of the observations (the ferry crosses the inlet each 30 minutes every day between 06.00 and 22.00 hrs) make the observations in principle very suitable for such studies.

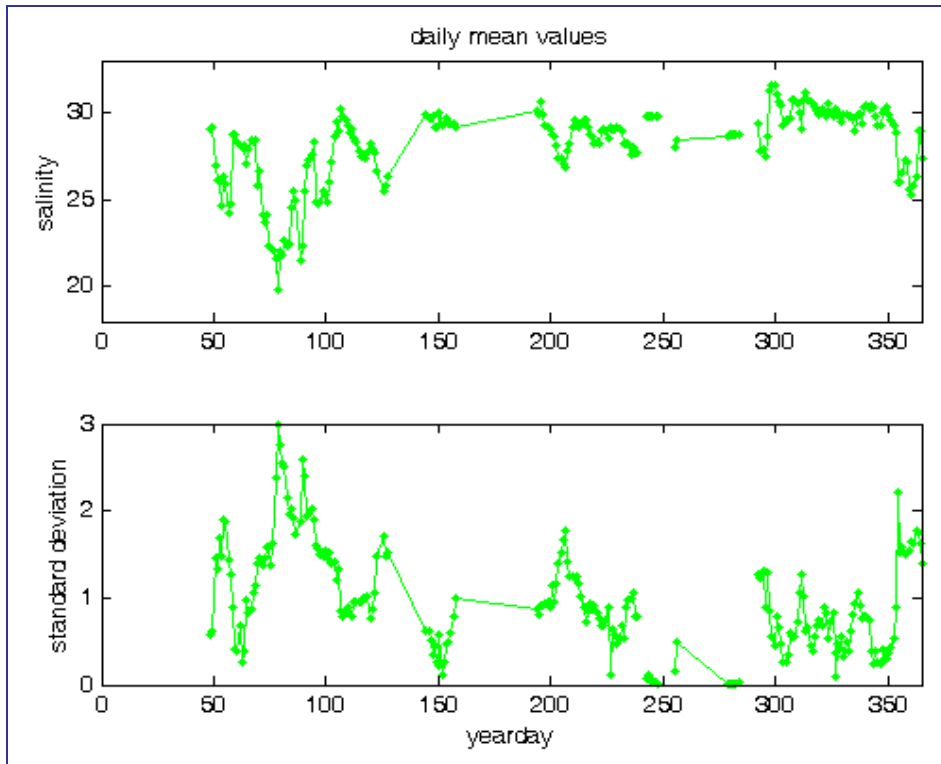


Figure I-9: Daily averaged salinity (top) and daily standard deviation (bottom) in the Masdiep tidal inlet for a period of one year.

Figure I-10 shows the monthly mean absolute value of the flux of suspended sediments through the Marsdiep tidal inlet for 2003, divided between flood and ebb periods. The difference between both indicates the net flux. There appears to be a relatively large net flux of suspended sediments towards the Wadden Sea. Moreover, this flux is substantially larger during spring and early summer, as compared to the other periods suggesting that biological processes play an important role in influencing the magnitude of this net flux (Ridderinkhof & Merckelbach, 2006).

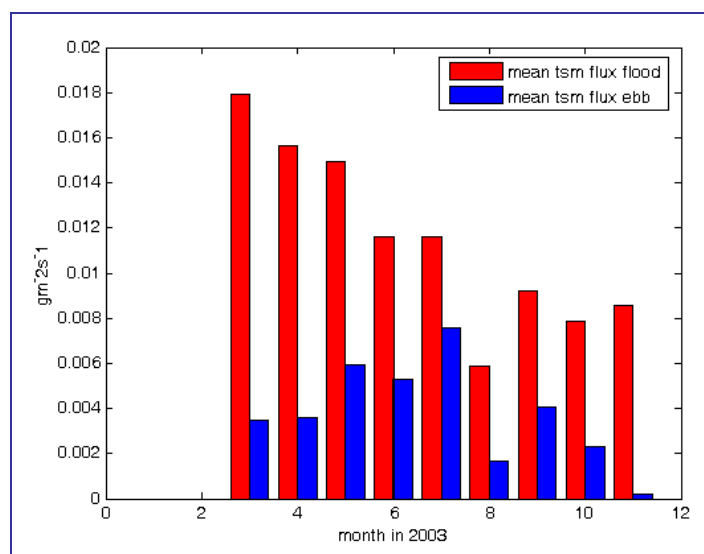


Figure I-10: The monthly mean flux of suspended sediments through the Marsdiep tidal inlet.

I-5 Identifying Upwelling Events along the Spanish Coast of the Bay of Biscay

Northwards of Santander there is a geographical coincidence of different sampling methods (Figure I-11). Firstly there is a standard section as part of the Radiales program from IEO (Spanish Institute of Oceanography). This program occupies monthly oceanographic sections around the Iberian Peninsula (Valdes et al., 2002). The Santander section began in late 1991 with Station 6 (labelled IEOS6) the best sampled oceanic station with 138 CTD profiles from May 1992 to May 2005. The track of the ferry “Pride of Bilbao”, which serves on the route Southampton – Bilbao, passes about 40 km from the IEOS6 twice a week throughout the year excluding a month for winter service.

A time series of Ferrybox measurements in the box adjacent to IEOS6 has been constructed (FBPoB) for use here. In addition, the area is covered by satellites measuring SST and ocean color. We will include a time series of SST in the grid cell centred at 44.5° N 3.5° W (referred to as OIRe02) from the weekly NOAA_OI_SST_V2 dataset.

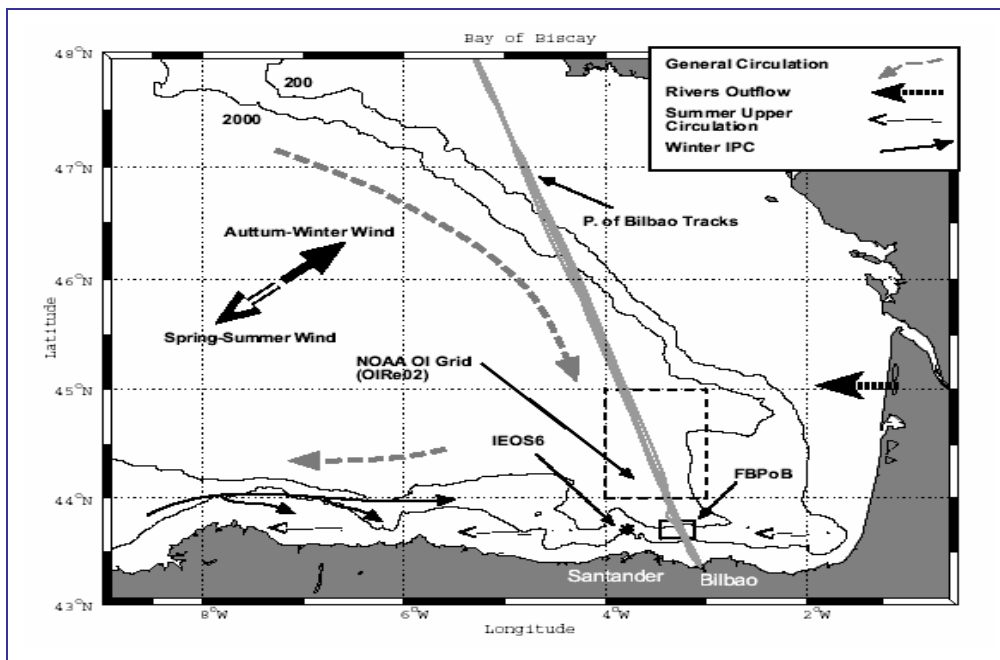


Figure I-11: Measurements used in the study.

The time series generated by the Pride of Bilbao consists of continuous underway data along a track which is traversed in both directions at intervals of a few days; therefore each position is sampled at intervals from 8 hours to 3 – 4 days. The time series FBPoB, given by the average SST when crossing the area nearby IEOS6 (Figure I-11) is compared to the OIRe02 and IEOS6 series in Figure I-12-A. The FBPoB series displays, as expected, the same seasonal cycle and is an independent source for generating such important timeseries all along the track of the line. The Ferrybox data also adds information at a temporal scale which is not captured either by the OIRe02 dataset or the IEOS6.

An example of this is shown in Figure I-12-B, spring and summer of 2004, which shows some abrupt cooling/warming events of the SST, some clearly related to the local wind forcing (indicated by arrows) but with others seemingly uncorrelated (and therefore their explanation must be sought in an advective cause).

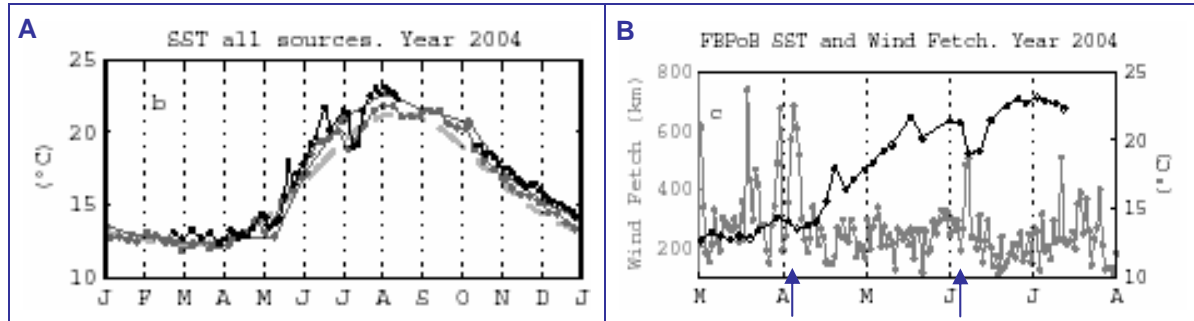


Figure I-12: A: SST annual cycle for 2004; B: FBPoB SST for spring/summer 2004 and wind fetch,

Salinity surface series (SSS) can be seen in Figure I-13. The main cyclical feature (IEOS6 series as solid lines with the annual harmonic in grey) which arises from the time series is the summer minimum and winter maximum values. This is mainly related to the surface circulation response to the wind pattern (an advective reason); during winter surface currents are predominantly eastward and carry salty water to the southeastern corner of the Bay of Biscay, in spring-summer the predominant winds are southwestwards and therefore surface currents are reversed bringing surface waters of low salinity, freshened in the previous spring, from the French rivers on the Biscay coast.

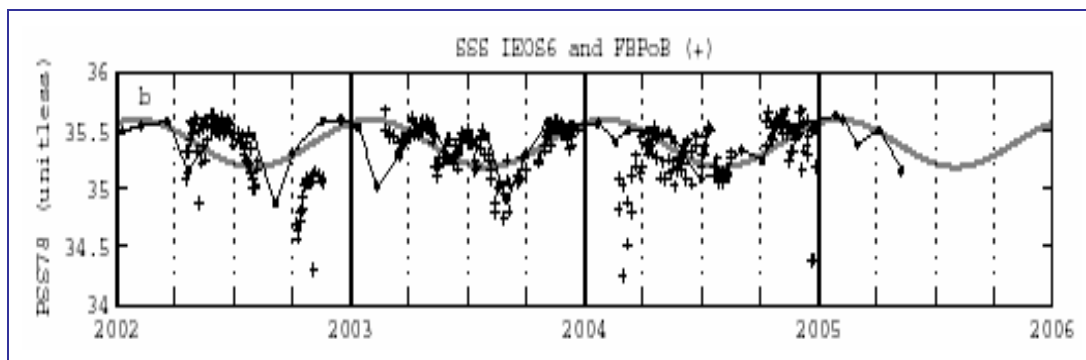


Figure I-13: Time series of surface salinity (SSS) from IEOS6 (solid lines) and FBPoB (+).

SSS time series from the FBPoB is a less robust parameter due to the bio-fouling and oil dirtying of the sensors, however, a consistent pattern is apparent, as demonstrated in the two salinity minima in the summers of 2002, 2003. An abrupt minimum in FBPoB found in winter to early spring 2004 came from a complex combination of local air-sea exchange and advection not properly captured up in IEOS6.

I-6 Impact of Tidal straining on Near Shore Salinity in Liverpool Bay

Temperature and salinity from the Birkenhead – Belfast ferry (Figure I-14) in 2004 have been examined to identify the tidal influence on near-shore salinity patterns.

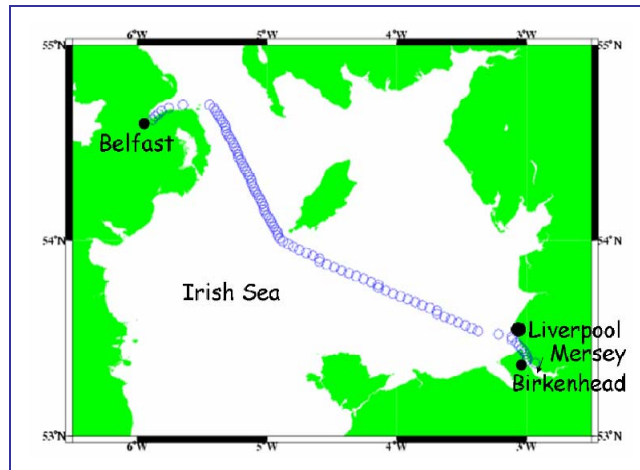


Figure I-14: Birkenhead to Belfast ferry track

The salinity time versus longitude plot shows distinct peaks of low salinity at the Liverpool end, corresponding to variations in the freshwater plume. There is no obvious direct correlation with river outflow data, but a comparison with tidal data (Figure I-15) strongly suggests that the variations correspond to mixing at spring tides followed by restratification at neap tides (e.g. lines indicated on Figure I-15).

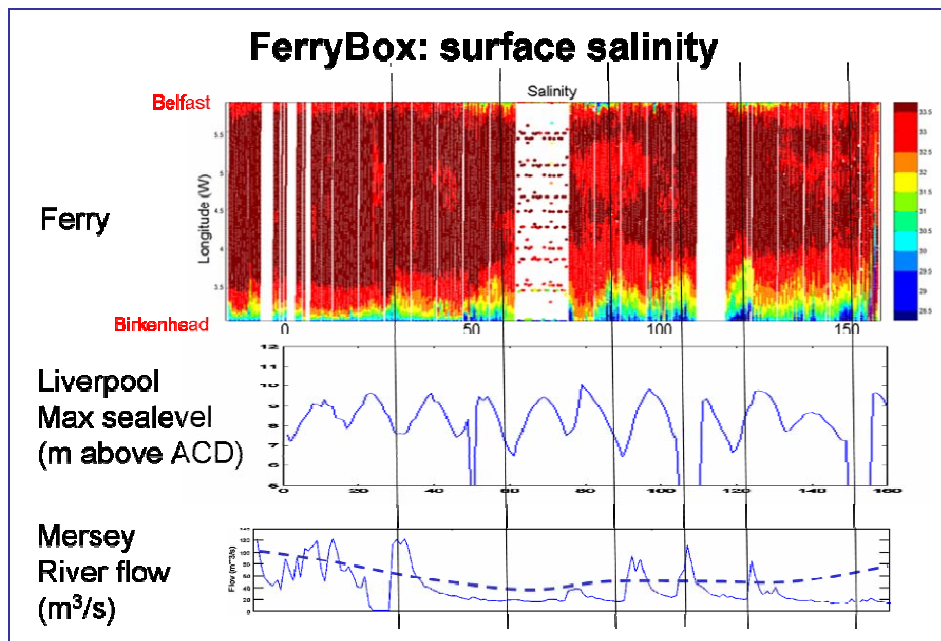


Figure I-15: Surface salinity measured aboard the Ferry for days 0 – 160 in 2004 (top), Liverpool sea level maxima (middle), Mersey river flow (bottom).



On occasions, though, neap tide and river flow peak appear to coincide. The variation in plume extent (several 10s of km) considerably exceeds the tidal excursion (total about 6 km due to M2 and 9 km at springs) which can also produce some variation in the apparent measured position of the plume. This stability cycle in Liverpool Bay has been observed by Sharples and Simpson (1995: Continental Shelf Research 15:295-314), but with a much shorter record.



I-7 Characterising Eco-hydrodynamic Regimes and Fronts in the Irish Sea

The characteristics of the different eco-hydrodynamic regions can only be fully determined if measurements last longer than a year, since the seasonal cycle is fundamental. The mean, standard deviation, minimum and maximum temperature for all the ferry tracks passing south of the Isle of Man for a two year period, between 15 December 2003 and 5 December 2005, are shown in Figure I-16.

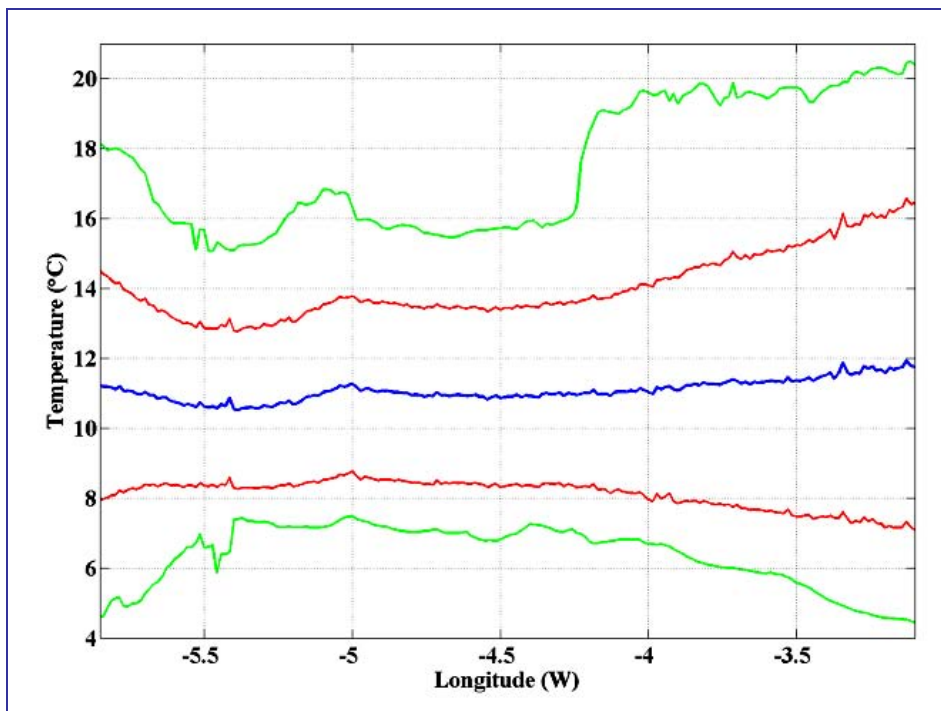


Figure I-16: Mean temperature (blue), mean \pm one standard deviation (red), maximum and minimum (green) for all crossings to Belfast the south of the Isle of Man between 15 December 2003 and 5 December 2005.

The pattern is largely as expected:

- A small but interesting variation of the mean, warmest (about 12 °C) in Liverpool Bay and Belfast Lough and coolest to the west of the Isle of Man, at 5° 25' W, less than 11°C. There is a local maximum (11.5 °C) at 5° W, south-west of the Isle of Man.
- The standard deviation (indicative of the seasonal cycle) is smallest in the deep water to the west of the Isle of Man and largest where the water is shallowest; in Liverpool Bay the annual temperature range is 1.4°C (Figure I-17).
- The most notable feature in the figure is the large change in the maximum temperature, about 3 °C, near 4° 15' W, north of Anglesey, indicative of significant temperature gradients.

These gradients, positive increasing towards the west, are shown in Figure I-17.

Concentrating on the Birkenhead to Belfast route south of the Isle of Man, as expected there were significant gradients close to the coast, particularly in Belfast Lough with temperature gradients in excess of $0.5\text{ }^{\circ}\text{C km}^{-1}$.

Of greater interest are the gradients away from the coast where there are three regions of gradient change:

- A Cooling westward at 4° W
- B Warming westward at 5° W
- C Cooling westward at $5^{\circ}\text{ }10'\text{ W}$.

The latter two (A & B) are a consequence of summer stratification to the west of the Isle of Man which results in a pool of warmer surface water, Horsburgh et al (2000).

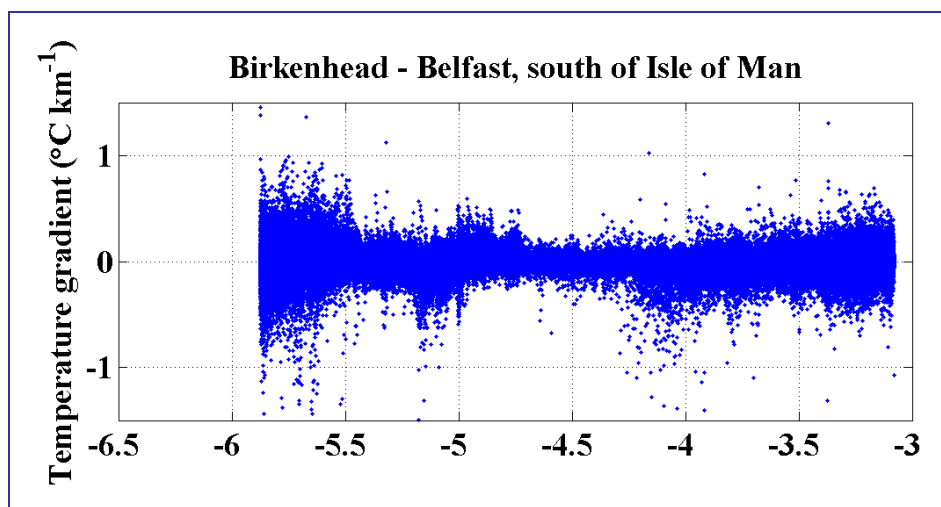


Figure I-17: Temperature gradients ($^{\circ}\text{C km}^{-1}$) from all the data on each route.

(B) arises as the ferry enters the pool (travelling westward) and (c) as it leaves; (a) is of more interest as it was not anticipated. Splitting the record into seasons and years the gradients here are present only in summer and are much more pronounced in 2005 compared with 2004, with values cooling westward in excess of 1° km^{-1} , Figure I-18. Note that there were only 46 crossings in 2005 compared with 138 in 2004.

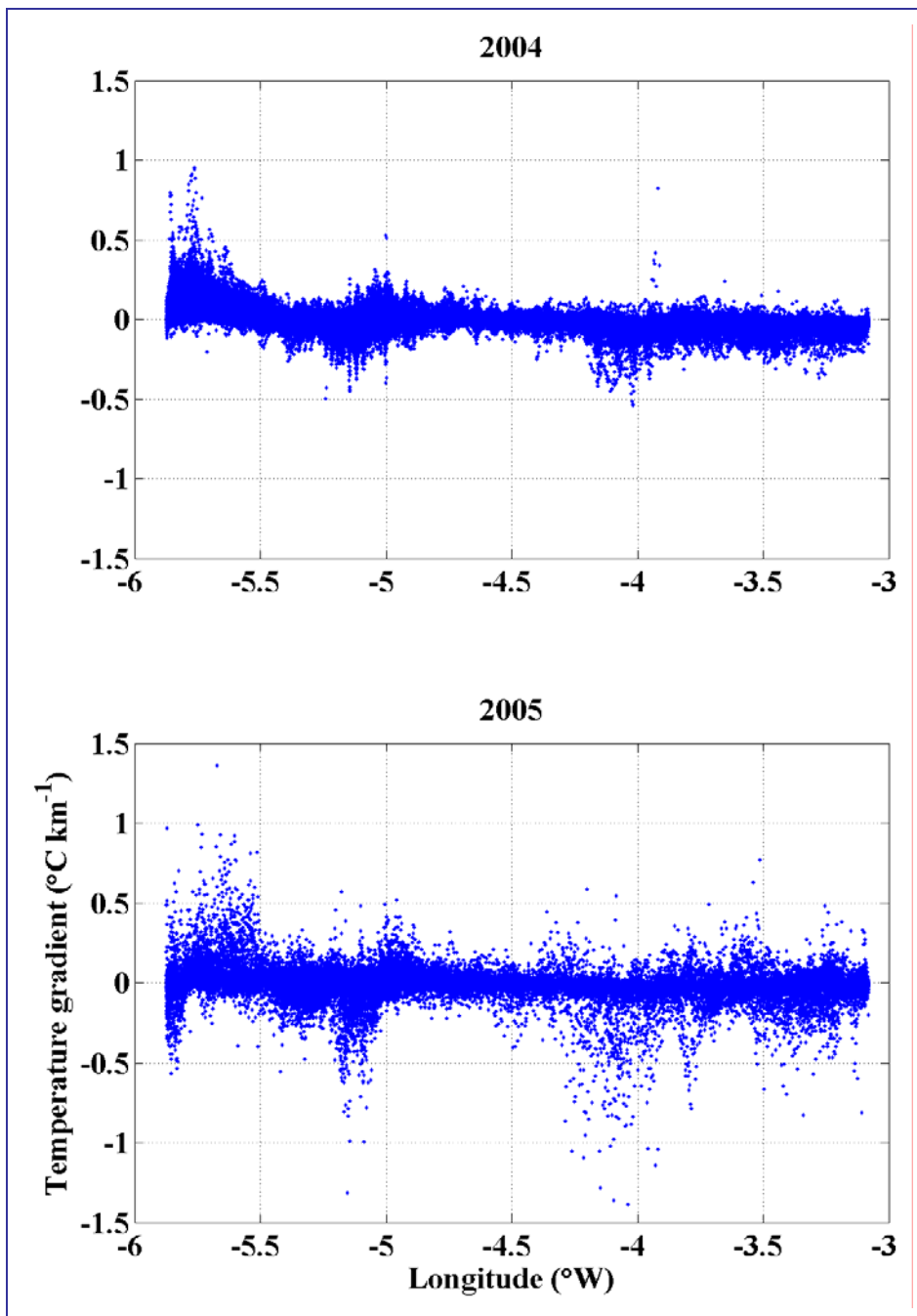


Figure I-18: Temperature gradients (°C km⁻¹) along the ferry route south of the Isle of Man in summer (July, August, September) for 2004 (top) and 2005 (bottom).

I-8 Air-Sea Interaction Evidenced by Ferrybox Measurements in the Aegean Sea

Ferrybox data can also be used to study air-sea interaction. The regularly scheduled ship-of-opportunity tracks (Figure I-19) can provide valuable information on the high frequency surface temperature variability driven by atmospheric events such as the passage of a storm.

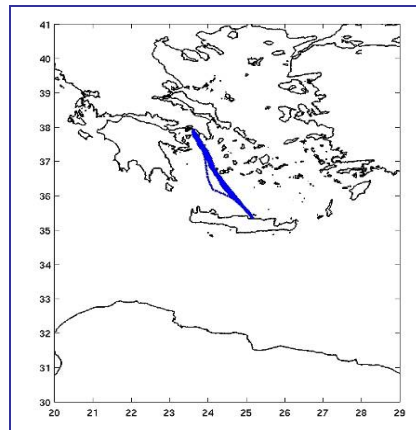


Figure I-19: Sample ferry tracks, Athens to Heraklion across the Aegean Sea.

This is illustrated in Figure I-20 showing the along track sea-surface temperature changes due to a snow storm over the Aegean Sea that occurred during the night of the 12 February 2004. A severe snow storm occurred during the night of 13 to 14 February 2004, during which the sailing of ferries was not allowed by the Hellenic Coast Guard. For this particular storm, it is estimated that the mixing after the storm was at least down to 200 metres of water depth. Therefore the Ferry-Box temperature measurements after the storm represented at least the upper 200 m of the water column. The general temperature drop in at least the upper 200 m layer due to the storm was in the order of 0.2-0.5 °C.

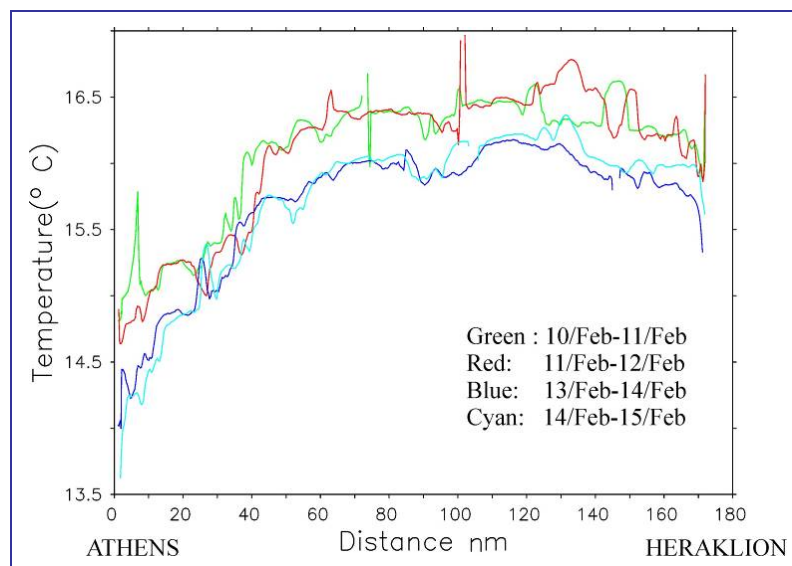


Figure I-20: Along-track space-series plots of surface temperature in the south Aegean Sea. Each trip lasts from the 21:00 hour (local time) to approximately 06:00 hour of the next day.



References for Part I

- Horsburgh, K.J., Hill, A.E., Brown, J., Fernand, L., Garvine, R.W., Angelico, M.M.P. (2000). Seasonal evolution of the cold pool gyre in the western Irish Sea. *Progress in Oceanography*, 46, 1-58.
- Hydes, D.J., C. P. Barger, B. A. Kelly-Gerrein, H. Wehde, W. Petersen, S. Kaitala, V. Flemming, K. Sørensen, J. Magnusson, I. Lips, and U. Lips 2006. Comparison of eutrophication processes and effects in different European marine areas based on the results of the EU FP-5 FerryBox Project. (*This volume?*)
- Kelly-Gerreyn, B.A., Hydes, D.J., Jégou, A.M., Lazure, P., Fernand, L.J., Puillat, I., García Soto, C. 2006. Low salinity intrusions in the western English Channel. *Continental Shelf Research*, in review.
- Laanemets, J., Kononen, K., Pavelson, J., Poutanen, E.-L., 2004. Vertical location of seasonal nutriclines in the western Gulf of Finland. *J. Mar. Syst.* 52,1-13.
- Laanemets, J., Lilover, M.-J., Raudsepp, U., Autio, R., Vahtera, E., Lips, I., Lips, U. 2006. A fuzzy logic model to describe the cyanobacteria *Nodularia spumigena* bloom in the Gulf of Finland, Baltic Sea, *Hydrobiologia*, 554: 31-45.
- Lips, I. 2005. Abiotic factors influencing the cyanobacterial bloom occurrence in the Gulf of Finland. *Dissertationes Biologicae Universitatis Tartuensis*, 108, 47 p., Tartu University Press.
- Ridderinkhof, H., Merckelbach, L. 2006. Suspended sediment fluxes through the Marsdiep tidal inlet from long-term ferry-ADCP observations. In preparation.
- Vahtera, E., Laanemets, J., Pavelson, J., Huttunen, M., Kononen, K., 2005. Effect of upwelling on the pelagic environment and bloom-forming cyanobacteria in the western Gulf of Finland, Baltic Sea, *J. Mar. Syst.* 58,67-82.
- Valdes, L., A. Lavin, M. L. Fernandez de Puellas, M. Varela, R. Anadon, A. Miranda, J. Camiñas, and J. Mas. 2002. Spanish Ocean Observation System. IEO Core Project: Studies on time series of oceanographic data, in *Operational Oceanography: Implementation at the European and Regional Scales*, edited by N. C. Flemming and N. Vallergera, pp. 99-105, Elsevier Science.



Part II The Role of Numerical Models in Understanding Processes Observed by Ferrybox Measurements

Numerical models operated by partners, GKSS, HYDROMOD, NERC.POL have been used to provide additional insight into the Ferrybox measurements. Three examples of their findings are presented here.

II-1 Understanding the Role of Advection in Interpreting Ferrybox Data in the Southern North Sea

The potential for Ferrybox data to precisely determine the connection between environmental significant processes and their physical and biogeochemical driving processes is a key question addressed within the project. As Ferrybox data sets are limited to the specific traces of the ferries additional information aside the routes, e.g. from fixed monitoring stations, is needed to resolve environmental characteristics with a broader spatial extension. However, simple comparison between the Ferrybox data and those from fixed stations often fails because of the predominant circulation pattern of the surrounding water masses.

The present study is therefore focussing on methodical aspects to resolve and display the fate of water measured with a Ferrybox. To derive more realistic comparisons between data from Ferryboxes and those from fixed monitoring stations, numerical models and Lagrangian tracer methods were employed to provide insight into the measurements from the GKSS Ferrybox system in the southern North Sea.

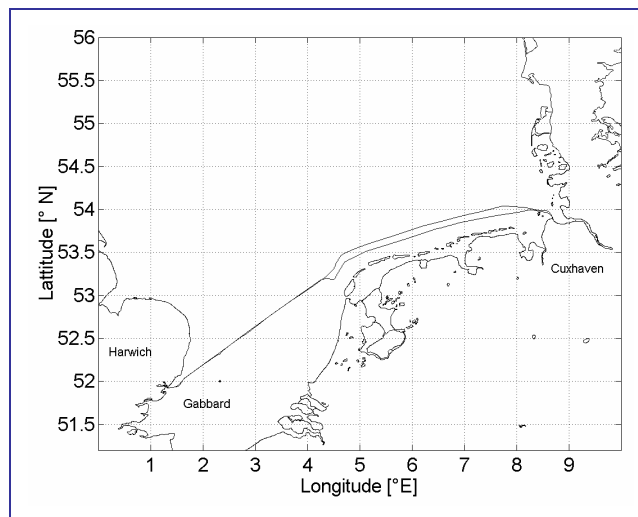


Figure II-1: Ferry track Cuxhaven – Harwich and position of the CEFAS Gabbard Bouy.

Two different observational data sets were used within this study, measurements from the German Ferrybox system installed on the Cuxhaven-Harwich ship of opportunity (Petersen et al., 2003, Wehde et al., 2003), and a spatially fixed buoy data set from the CEFAS Gabbard Bouy, both shown in Figure II-1.

The latter forms part of the National Marine Monitoring Programme (NMMP) of the UK. The measured parameters available from the Ferrybox are salinity, pH, oxygen, turbidity, fluorescence, ammonium, nitrate/nitrite, o-phosphate and silicate.

The buoy data comprise of phytoplankton concentration, conductivity, temperature, suspended sediment concentration and light penetration. For this study salinity and Chlorophyll Fluorescence were compared to buoy data during spring/summer in 2002.

The GKSS models applied for this study consists of a general circulation model (GCM), a Lagrangian Tracer model and a primary production module. The GCM used a two dimensional triangle grid and is forced with variable wind, tides and Coriolis force. A coupled nesting is applied for the estuary regions with highest resolution of the model in the southern German Bight (80 m) and lowest resolution of the model in the Northern North Sea (3 km) (Plüß, 1999).

Water parcels measured with the Ferrybox were introduced as Lagrangian Tracers into the GCM in order to simulate the geographical displacement. To simulate the temporal development of non-conservative tracers like the chlorophyll the primary production module is implemented for each of the tracers (Wehde et al., 2001).

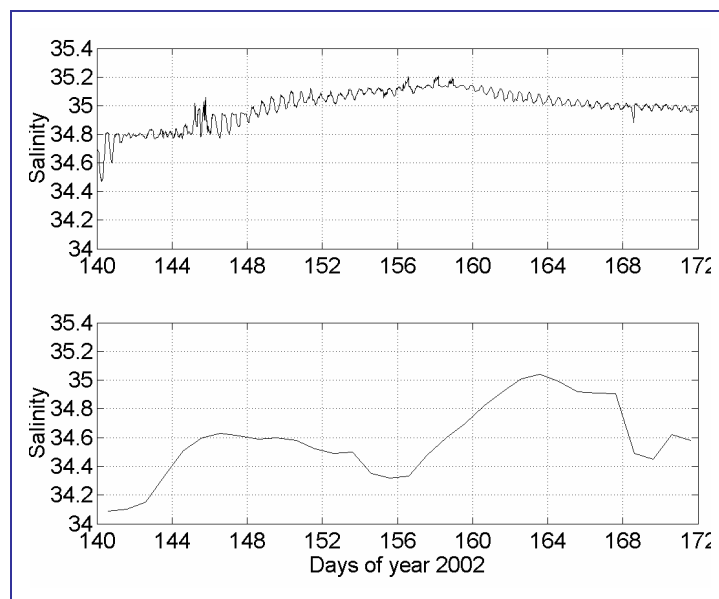


Figure II-2: Comparison between Salinity data from CEFAS Gabbard Buoy (upper panel) and Ferrybox data (lower panel) using from the nearest geographical point of the route to Gabbard station.

The results for the comparison between the modelled salinity tracer data from the CEFAS Gabbard Buoy and those from the Ferrybox are displayed in Figure II-2. As can be seen there is little agreement.

With the implementation of the Lagrangian tracers into the GCM the main characteristics of the different datasets are now in good agreement (Figure II-3). The salinity anomaly observed in the Ferrybox data set can be explained by entrainment of surrounding water masses on the way from the Gabbard buoy up to the ferry line.

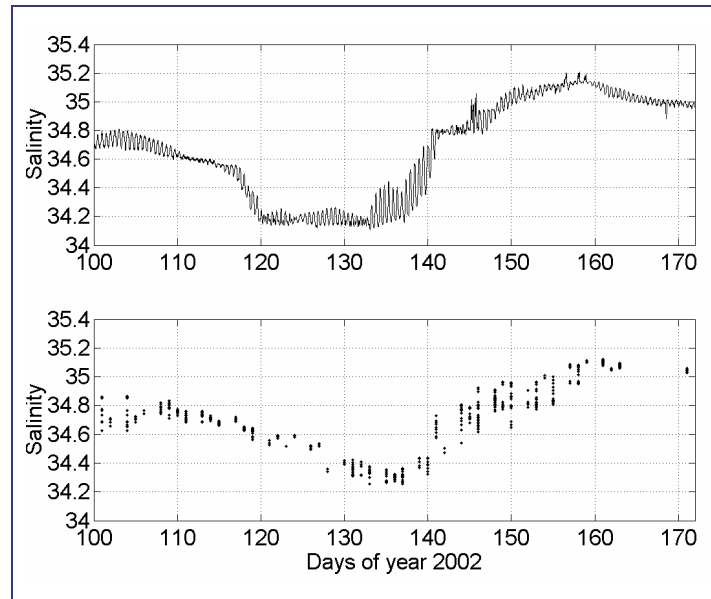


Figure II-3: Comparison of salinity data measured at CEFAS Gabbard Buoy (upper panel) with salinity data from passively tracers, observed with the Ferrybox and transported within the GCM (lower panel).

The time the water parcels need for their travel from the Gabbard Buoy to the Ferry line is displayed in Figure II-4. Beginning with relatively long travel times during early spring the travel times are decreasing until the second half of May (~ day 140). With the start of the building of a seasonal thermocline the transport velocity decreases again and the water needs more time to be advected from the Gabbard Buoy up to the ferry line for the rest of the period.

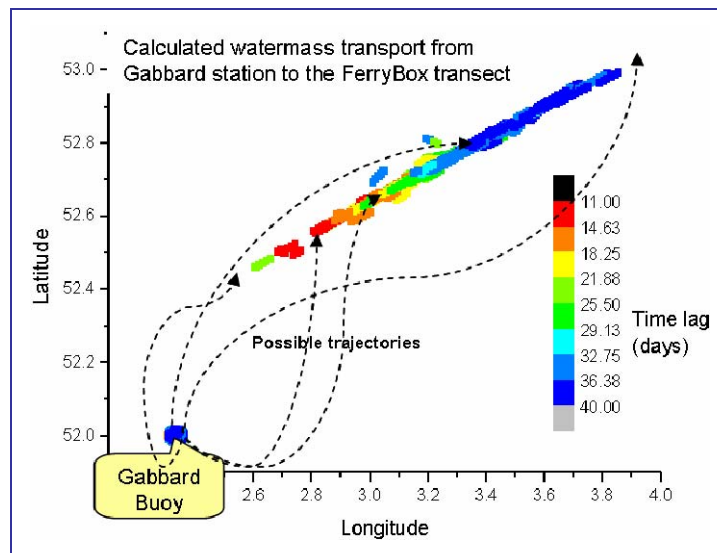


Figure II-4: Travel times for water parcels leaving the Gabbard Buoy.

While the results for salinity are explained by the use of Lagrangian tracers, using these conservative tracers for non conservative parameters like chlorophyll fluorescence remains strongly unsatisfactory (Figure II-5).

Although the data displayed are thought to be the same water mass the results are very different. None of the characteristics of the Gabbard Buoy data set can be observed within the simulated Ferrybox data set.

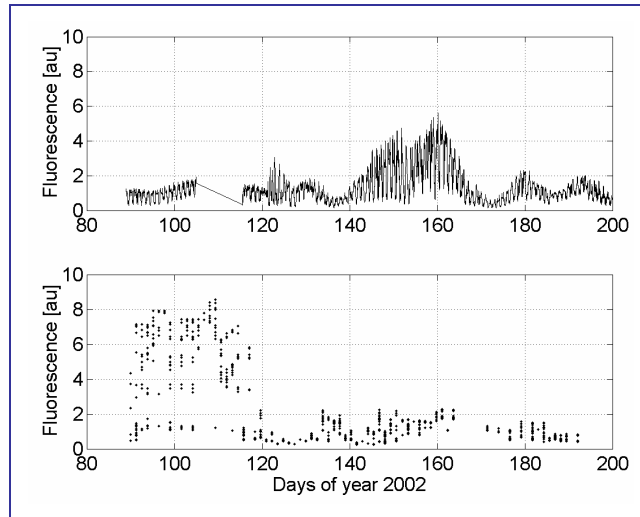


Figure II-5: Chlorophyll fluorescence observed at CEFAS Gabbard buoy (upper panel) and chlorophyll fluorescence of water passively transported within the GCM (lower panel).

By applying the Chlorophyll module for the Lagrangian tracers, taking the measurements from the Gabbard Buoy as initial values and forcing the simulations with realistic light conditions and the nutrient distribution measured at the Gabbard Buoy the results for the non conservative parameter chlorophyll fluorescence are considerably better (Figure II-6). All the characteristics of the different data sets are now estimated in good agreement. The bloom feature observed at the Gabbard Buoy decays on the way northwards to the ferry track due to the lack of sufficient nutrient. The bloom feature that occurs in the Ferrybox observations is developed from the initial low chlorophyll values of the Gabbard Buoy measurements through production that continues during the period the water is transported from the Buoy to the ferry track.

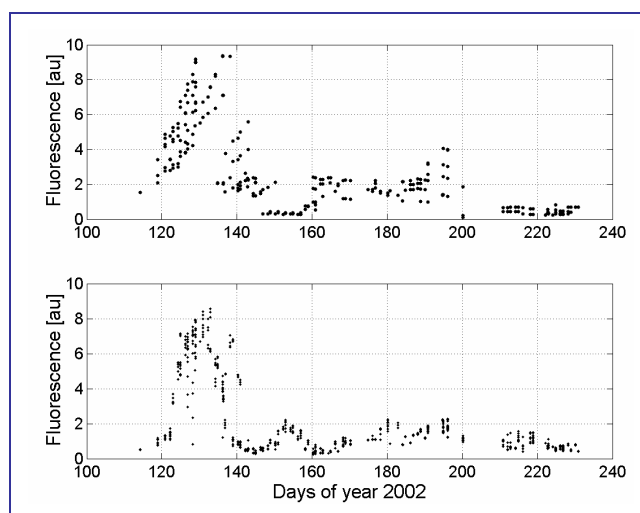


Figure II-6: Comparison between observed Ferrybox Chl Fluorescence (dots) and estimated chlorophyll for tracers starting from the CEFAS Gabbard Buoy and drifting to the ferry route (crosses).

II-2 Understanding the Spatial Extent of Waters Sampled by Ferrybox Measurements in the Southern North Sea

Employing a similar modelling approach to GKSS above, HYDROMOD adapted a three-dimensional baroclinic current model derived from the shallow water equations using a numerical algorithm (a semi-implicit scheme) proposed by Backhaus (1983), subsequently modified by Duwe and Hewer (1982) to a two-step method to cope with special shallow water features like strong non-linearities in the current field and the wetting-drying processes in inter-tidal areas.

A Lagrangian tracer model (*HYDROMOD-TRACER*) was applied to investigate transport and dispersion processes in two- or three-dimensional shallow and deep water applications. The tracer methodology is based on the description of substance distributions by a large number of particles within a flow field ('marker-and-cell' method, Harlow and Welch, 1965; Maier-Reimer and Sündermann, 1982; Duwe, 1989).

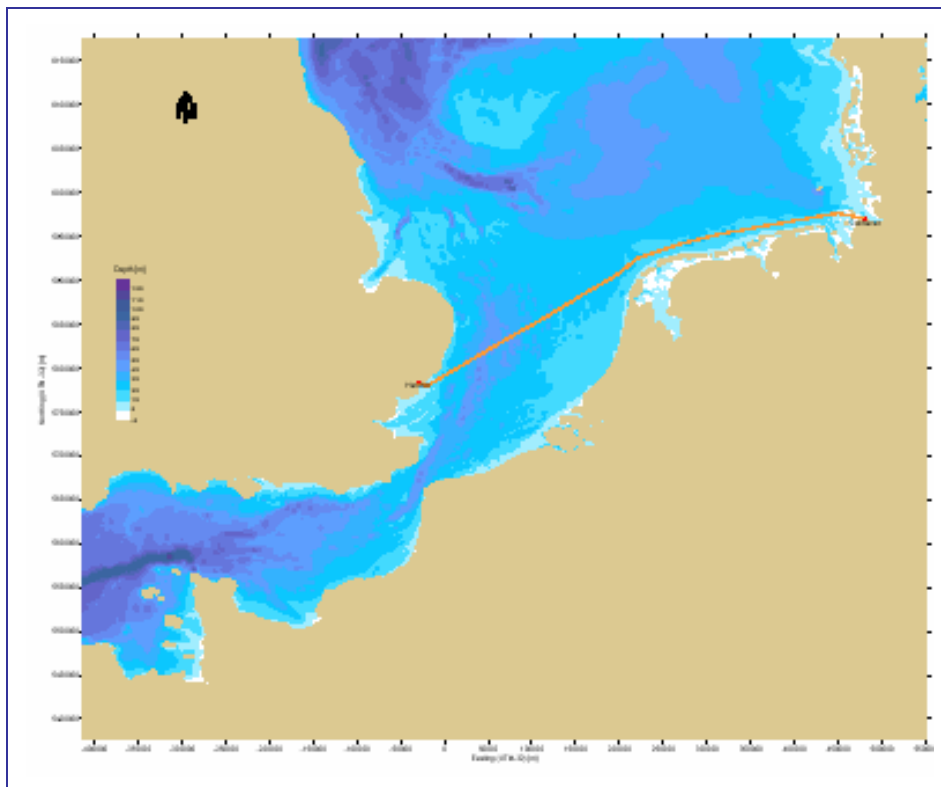


Figure II-7: Model domain, bathymetry and ferry track Cuxhaven – Harwich.

The model domain covers the southern North Sea from Blåvands Huk (Denmark) to the Western entrance of the English Channel (see Figure II-7) with an equidistant grid spacing of 617.333 m (1/3 of a nautical mile). The topography is based on the UTM-32 'Bathymetry of North Sea, Baltic Sea and Connecting Seas', April 2003, purchased at the Danish Hydraulic Institute (DHI). In addition more accurate bathymetric data for the Channel region was provided by NERC.POL (R. Proctor) and for the Dutch coast by NIOZ (H. Ridderinkhof). Open boundary and initial conditions were provided by the larger area, coarser resolution BSH model and surface wind forcing by the German Weather Service (DWD) together with the data from the operational BSH model system.

Model process studies have shown the way of combining Ferrybox information with tracer algorithms to look at phenomena like the movement of coastal fronts and mixing of water masses. In a first step the spring-neap tidal modulation and its effect on water mass transport and mixing have been investigated by releasing an ensemble of tracers and following their pathways. The fate of the water masses represented by the tracers shows that the distribution even after a few days is highly dependent on the hydrographic situation (see Figure II-8). This fact, however, proves that the area indirectly covered by Ferrybox information may be relatively extensive in periods of spring tides or storm events.

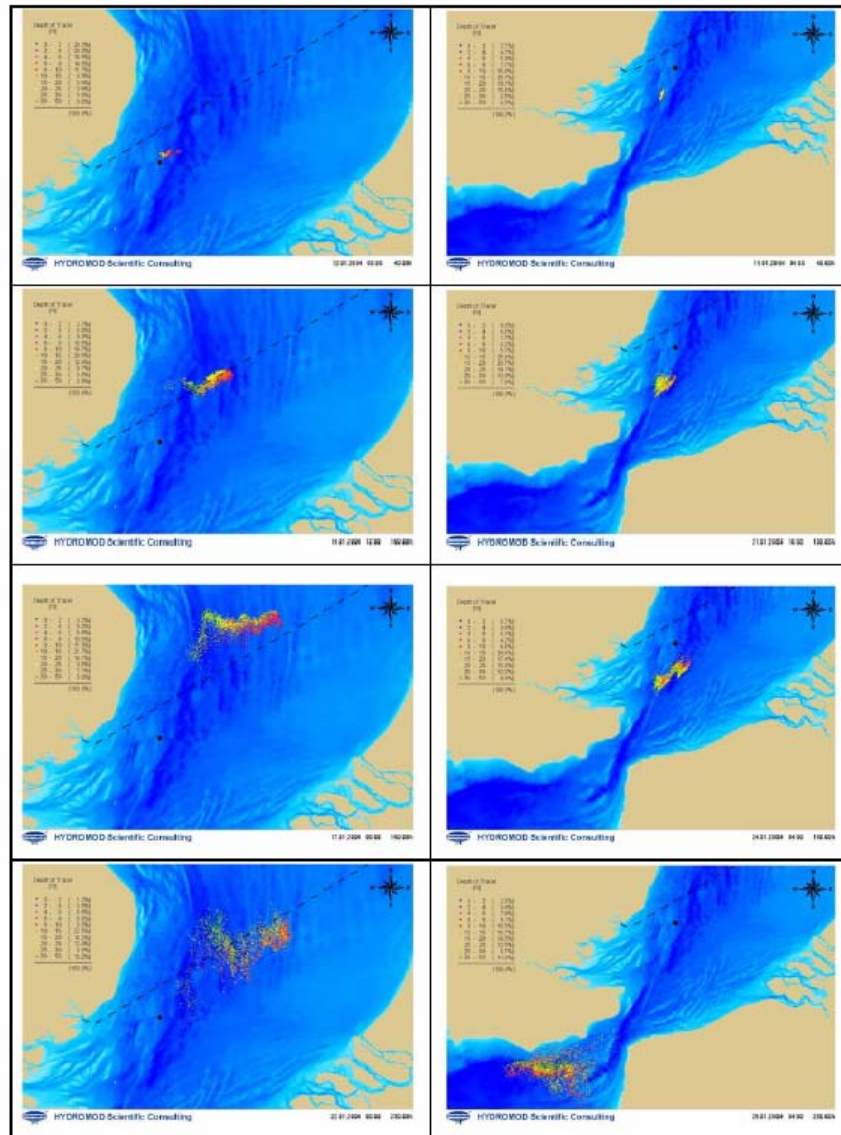


Figure II-8: Simulated tracer distributions after different time steps (colour of particles depicts their depth). Left: release at spring low water Harwich, right: release at neap low water Harwich. (Black dot: release position W. Gabbard Buoy; dotted line: ferry track).

Further experiments to examine the spread of waters crossed by the ferry have been conducted. Figure II-9 shows the spatial distribution of tracers which were released at different positions along the ferry track between 16 and 24 April, 2005 together with their salinity characteristics (left), and the resulting “coverage” of Ferrybox information (right).

We can see from these figures that the extent of “ferry water” can be seen as far as 50 km from the ferry track within 8 days.

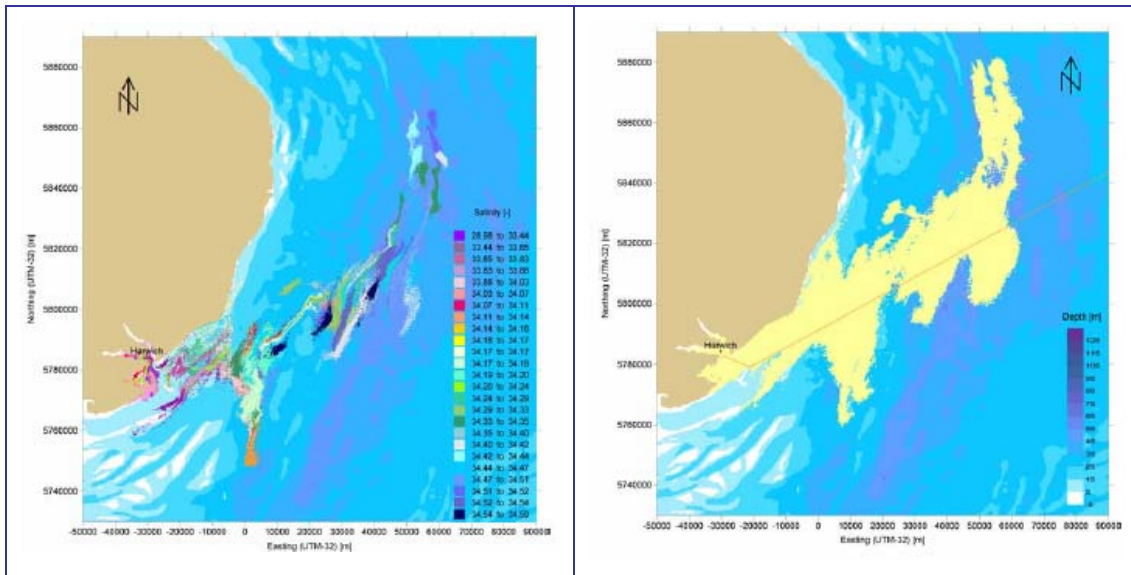


Figure II-9: Coverage with tracers released off Harwich along the ferry track at different times and collected over several days.

Output from a second case study is given in Figure II-10. Here tracers were released every 5 minutes between 0510 and 0700 UTC on 18 April and collected every six hours between 0600 UTC 18 April, and 1800 UTC 22 April 2005.

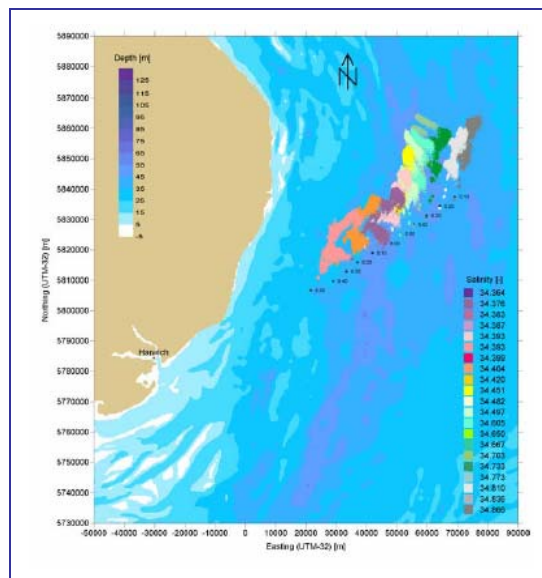


Figure II-10: Characteristic salinity of a different tracer field.

In this example, because of the different release pattern and different tidal and meteorological forcing, we see a different spreading (and mixing) pattern. Understanding the spread of water masses around the ferry route is an extremely useful aid to interpret the measurements and can act as a guide to the de-correlation length scales to be applied if the Ferrybox measurements were to be assimilated into numerical models.

II-3 The Irish Sea: Modelling the Long-term Variability of Temperature and Salinity in the Irish Sea: Implications for Ferrybox Measurements

It is seen that horizontal gradients in salinity drive an estuarine-like residual circulation in the eastern Irish Sea (Czitim, 1986), and vertical gradients in salinity allow stratification to develop near freshwater sources inshore, such as Liverpool Bay (Sharples & Simpson, 1995). In the western Irish Sea, although salinity contributes to the early development of stratification near the Irish coast, once stratification is developed it plays a relatively minor role, with the temperature dominating the seasonal stratification (Horsburgh et al., 2000). Throughout the year the horizontal salinity distribution in the western Irish Sea shows more saline waters in the deep central region, decreasing westwards with minimum values near the Eastern Irish Sea coast (Bowden, 1980). Detailed cruise data indicate a sharp transition between the fresher coastal waters and more saline Irish Sea waters (e.g. Jones & Folkard, 1971), the location of which is driven by climatic influences such as river discharge and the strength and salinity of Celtic Sea inflows (Evans et al., 2003).

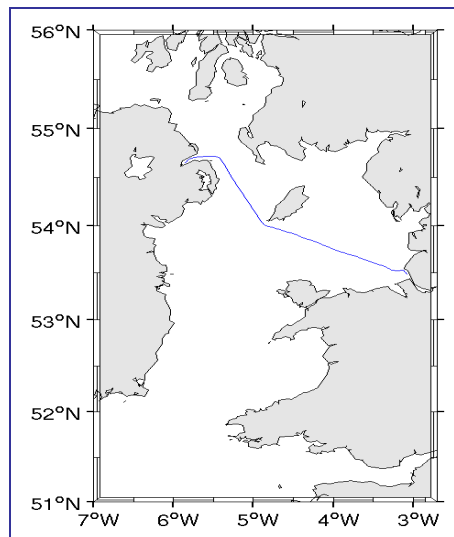


Figure II-11: Map showing model domain and standard Birkenhead to Belfast ferry route.

The Birkenhead to Belfast ferry, operated by Norsemerchant (www.norsemerchant.com) passes through all these hydrographic domains making it an ideal instrument for spatially sampling the Irish Sea.

The Proudman Oceanographic Laboratory Coastal Ocean Modelling System (*POLCOMS*) is a three-dimensional finite difference primitive equation model (described by Holt and James, 2001) formulated in spherical coordinates on an Arakawa (1972) B-grid with a terrain following sigma coordinate system in the vertical. Key aspects of the numerical scheme include: calculation of vertical diffusivities for momentum and scalars using a Mellor-Yamada-Galperin level 2.5 turbulence closure scheme; calculation of horizontal pressure gradients by interpolation onto horizontal planes, which significantly reduces the numerical errors commonly found over steep topography in sigma-coordinates; and use of the 'Piecewise Parabolic Method' (PPM), (James, 1996) for horizontal advection of physical variables, which is a conservative scheme that minimizes numerical diffusion and has excellent front preserving properties.

The ability of this model to reproduce the observed barotropic and baroclinic variability on the northwest European shelf has been demonstrated in a range of applications, including Proctor and James (1996), Holt and James (2001), Holt et al. (2001) and Holt and Proctor (2003).

In this study, the model grid has a horizontal resolution of $1/20^\circ$ longitude by $1/30^\circ$ latitude, and has 25 layers in the vertical distributed evenly throughout the water column. The domain is from 7° W to 2.65° W, and from 51° N to 56° N, thus extending into the Celtic Sea in the south and beyond the North Channel of the Irish Sea in the north (Figure II-11). Model bathymetry was obtained by smoothing a fine resolution (approximately 1 km) bathymetry digitized from Admiralty Fair Sheets (where available) and Admiralty Charts supplied by the U.K. Hydrographic Office (Brown et al., 1999).

The initial temperature and salinity fields were derived from winter climatologies for the northwest European shelf. At the open boundary, the model uses elevations and depth mean currents for 15 tidal constituents interpolated from an analysis of theNERC.POL Northeast Atlantic Model. Hourly residual elevations and currents, which represent the far field forcing, are taken from a simulation of theNERC.POL Storm Surge Model (Flather et al., 1991) for the 1960 – 1999 period. This simulation uses 6 hourly atmospheric pressures and surface winds from the Norwegian Meteorological Office (DNMI). Therefore to ensure consistency with the residual elevations and currents imposed at the open boundary, surface atmospheric pressure and wind fields for the present model are also spatially and temporally interpolated from the DNMI data. Spatially and temporally varying air temperature, relative humidity and cloud cover are interpolated from 6 hourly data provided by the National Centres for Environmental Prediction (NCEP, <http://www.cdc.noaa.gov>). Surface heat fluxes are then calculated using the bulk formulae discussed in Gill (1982). Short wave solar radiation is calculated from equations describing the dependence of solar radiation on the position of the sun, adjusted for cloud cover (as described in *COHERENS* user documentation, Luyten et al., 1999).

Temperature and salinity open boundary conditions are specified by an averaged annual cycle taken from a 5y (1998 – 2002) simulation of theNERC.POL Northeast Atlantic Model. Although the use of a modelled average annual cycle from a short period is not ideal, there are insufficient observational data available with which to derive spatially and temporally varying boundary forcing for the model. The potential impact of the representation of the open boundary salinity and temperature on model results is discussed in Young & Holt (2005).

For accurate simulations of salinity it is important to adequately represent freshwater inputs from precipitation and river flows. There are insufficient long term rainfall data to derive spatially varying precipitation fields for the forty year hindcast simulation. Instead daily precipitation rates are estimated by averaging the available data from 10 sites around the Irish Sea coast. Evaporation rates are calculated using the evaporative loss term of the bulk heat flux formulae.

Previous applications of *POLCOMS* to the northwest European shelf region have used daily discharge data from a small number (36) of European rivers to provide the freshwater riverine inputs (e.g. Holt and James, 2001). This is seen as inadequate for accurately modelling the salinity in the Irish Sea and use here is made of the dense network of gauging stations (currently around 1400) around Britain. However, the density of these stations varies considerably from region to region with relatively few stations in remote (e.g. western Scotland) or technically more challenging areas (e.g. in the flat terrain of East Anglia). Thus direct measurements account for only around 65% of the outflow from Great Britain.

To obtain a more accurate representation of freshwater flows, some estimate of the contribution from the ungauged areas is required, including consideration of major rivers in ungauged basins, minor streams draining directly to the sea, groundwater outflows, and in a few areas (e.g. the Thames estuary) sewage effluent. Researchers at the Centre for Ecology and Hydrology (CEH), Wallingford, have developed an adjustment technique based on the observed association between river flow and catchment size (Marsh and Sanderson, 2003). In summary, the method requires the identification of basic areal units for which outflows need to be aggregated, known as Hydrometric Areas (HAs); 97 HAs have been identified for mainland Britain. For each of these, representative index catchments are identified and weighting factors are derived to allow for those outflows that are not measured. These take the initial first-order estimates of runoff based on catchment size and further refine them by weighting according to the relation between mean runoff from the gauged and ungauged areas. The resulting weighting factors are used as multipliers for the gauged river data. Daily data for the full 40 year period are not available for all the gauged rivers, so a mean annual cycle is calculated from the available data and used to fill any gaps.

The model simulation is conducted for the period 1960-1999 in free running mode, i.e. this model does not use a relaxation to seasonal climatology. The ability of the model to accurately reproduce the long term variability of temperature and salinity is assessed by comparison with data and reported in Young & Holt (2005).

Here we concentrate on examining the outputs along the ferry track, shown in Figure II-11. However, some summary statistics to assess the quality of the model run are given in Table II-1, which indicates the excellent agreement between observed and modelled temperatures and the acceptable (for the present time) agreement between observed and modelled salinities (see Young & Holt (2005) for a discussion on this, which points to the large scale ocean forcing as the major source of error).

Table II-1: Statistical comparison of observed temperatures and salinities and the corresponding predicted values for the simulated period, 1960 – 1999 (3397 CTD profiles). Results presented as mean error and root mean square (RMS) error.

Temperatures	Mean (°C)	RMS (°C)
All points	-0.01	0.78
Near-surface	-0.08	0.71
Near-bed	0.00	0.86

Salinities	Mean	RMS
All points	0.79	0.98
Near-surface	0.81	0.99
Near-bed	0.78	0.96

Using all available CTD data (3397 profiles), the model reproduces the observed seasonal and longer term cycles in temperature, with mean and RMS errors of -0.01 °C and 0.78 °C. The temperature variability recorded at Cypris station is also well reproduced (Figure II-12). Model predictions of salinity are less accurate, and generally too saline, with mean and RMS errors of 0.79 and 0.98. However, whilst absolute values are not particularly well predicted many of the trends in the salinity variability observed at Cypris station are reproduced (Figure II-13), suggesting that many of the dominant physical processes influencing salinity variability in the Irish Sea are well represented in the model.

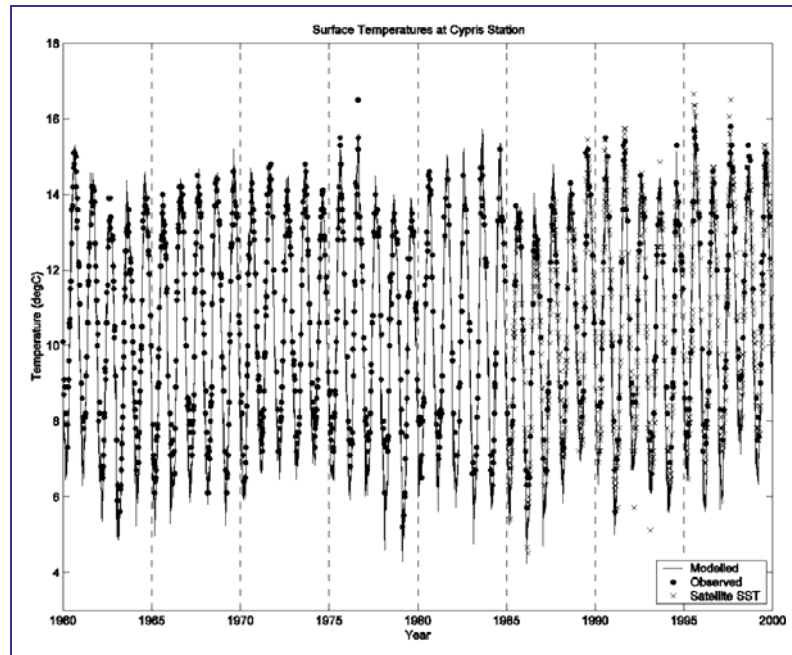


Figure II-12: Comparison of predicted and observed near-surface temperatures at the Cypris station over the period 1960-1999.

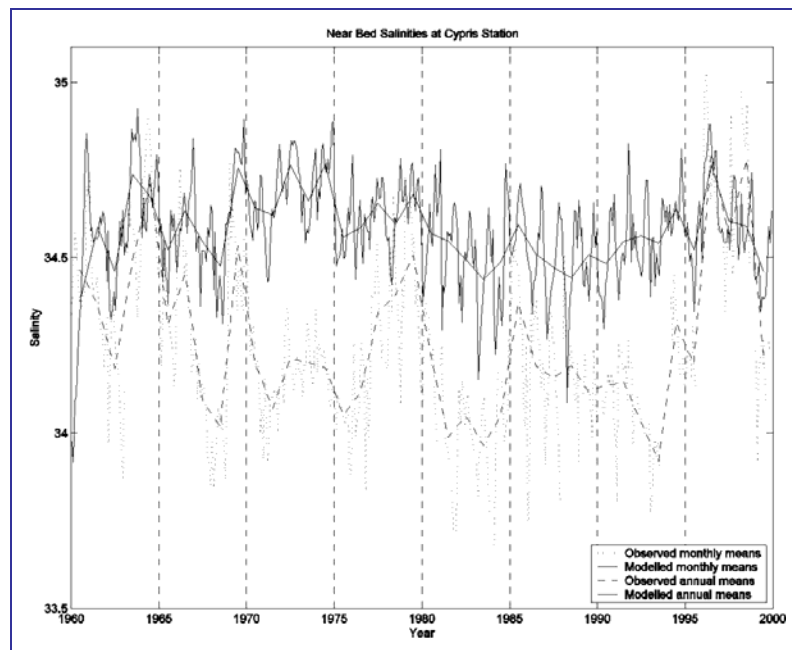


Figure II-13: Comparison of predicted and observed mean monthly, and mean annual near-bed salinities at the Cypris station over the period 1960 – 1999.

Temperature and salinity along the ferry track were extracted at daily intervals from the 40y run. These data were then averaged per month (i.e. all January tracks were collated) to produce a mean seasonal cycle and a monthly standard deviation. Figure II-14 and Figure II-15 show the mean and standard deviation for temperature and salinity respectively. Both indicate a mean seasonal cycle: in temperature this occurs predominantly across the whole track indicating the local effect of the seasonal heating and cooling cycle with some local enhancements close to both coasts.

In salinity there appears no such cycle, however, seasonal changes in salinity are seen close to both coasts with lower salinities in the winter than in summer. There appears no seasonal cycle in the standard deviation of temperature except in May, which correlates with the onset of stratification in the region west of the Isle of Man; maximum temperature standard deviation is 1.4 °C with strong along-route variability. Salinity standard deviation does have a seasonal cycle indicating that winter run off, especially in Liverpool Bay, can be variable; maximum salinity standard deviation is 2.5.

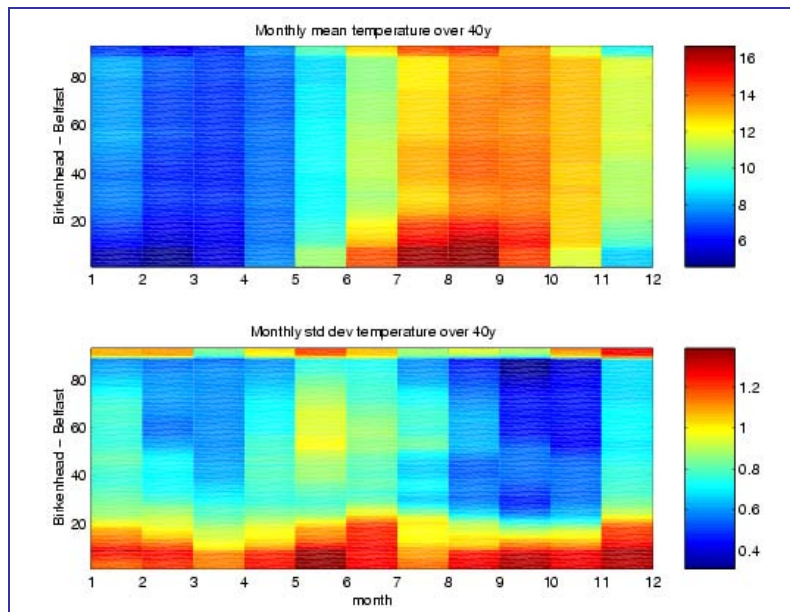


Figure II-14: Temperature along ferry route: 1960-1999. Y-axis: model gridpoints.

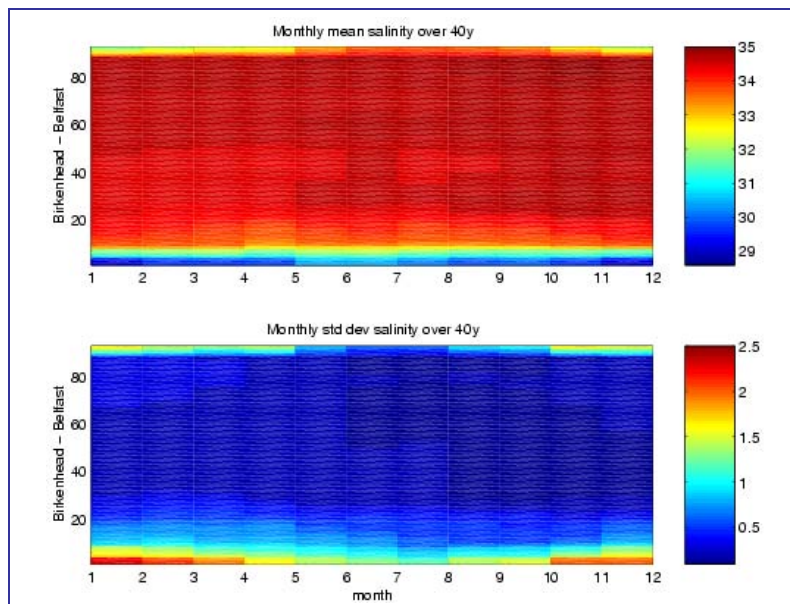


Figure II-15: Salinity along ferry route: 1960-1999. Y-axis: model gridpoints.

This shows the kind of variability we should expect to see in the Ferrybox measurements in the Irish Sea and indicates the expected range of variability.



Acknowledgement

This work partially supported by NERC grant NER/A/S/2001/00559.

References for Part II

- Arakawa, A. 1972. Design of the UCLA general circulation model. *Tech. Rep. 7*, Univ. of Calif., Los Angeles.
- Backhaus J. O. 1983. A semi-implicit scheme for the shallow water equation for application to shelf sea modelling. *Continental Shelf Research*, 2:243-254.
- Bowden, K.F. 1980. Physical and Dynamical Oceanography of the Irish Sea. In 'The North-West European Shelf Seas: The Sea Bed and the Sea in Motion II. Physical and Chemical Oceanography, and Physical Resources', F.T. Banner, M.B. Collins, K.S. Massie (eds.), Elsevier Oceanography Series, 24B, Elsevier Science Publishing Company, Amsterdam, pp. 391-413.
- Brown, J., Joyce, A.E., Aldridge, J.N., Young, E.F., Fernand, L., Gurbutt, P.A., 1999. Further identification and acquisition of bathymetric data for Irish Sea modelling. DETR research contract CW0753.
- Czitrom, S.P.R. 1986. The effect of river discharge on the residual circulation in the Eastern Irish Sea. *Continental Shelf Research*, 6 (3), 475-485.
- Duwe, K. C. 1989. Modellierung der Brackwasserdynamik eines Tideästuars am Beispiel der Unterelbe. *HYDROMOD Publ. no. 1*.
- Duwe K. C., Hewer, R. R. 1982. Ein semi-implizites Gezeitenmodell für Wattgebiete. *Deutsche Hydrogr. Zeitschrift* 35.
- Evans, G.L., Williams, P.J. le B., Mitchelson-Jacob, E.G. 2003. Physical and anthropogenic effects on observed long-term nutrient changes in the Irish Sea. *Estuarine, Coastal and Shelf Science*, 57, 1159-1168.
- Flather, R.A., R. Proctor, J. Wolf 1991. Oceanographic forecast models. In: *Computer Modelling in the Environmental Sciences*, D.G. Farmer and M.J. Rycroft, editors, IMA Conference Series 28, Clarendon Press, Oxford, pp.15-30.
- Gill, A.E. 1982. *Atmosphere-Ocean Dynamics*. Academic Press, New York, 662pp.
- Harlow F. H., Welch, J. E. 1965. The MAC method: a computing technique for solving viscous, incompressible, transient fluid flow problems involving free surfaces. *Phys. Fluids* 8.
- Holt, J.T., James, I.D. 2001. An s coordinate density evolving model of the northwest European continental shelf 1, Model description and density structure. *Journal of Geophysical Research* 106 (C7), 14015-14034.
- Holt, J.T., Proctor, R. 2003. The role of advection in determining the temperature structure of the Irish Sea. *Journal of Physical Oceanography*, 33, 2288-2306.
- Holt, J.T., James, I.D., Jones, J.E. 2001. An s coordinate density evolving model of the northwest European continental shelf 2, Seasonal currents and tides. *Journal of Geophysical Research*, 106 (C7), 14035-14053.
- Horsburgh, K.J., Hill, A.E., Brown, J., Fernand, L., Garvine, R.W., Angelico, M.M.P. 2000. Seasonal evolution of the cold pool gyre in the western Irish Sea. *Progress in Oceanography*, 46, 1-58.
- James, I.D. 1996. Advection schemes for shelf sea models. *Journal of Marine Systems* 8, 237-254.





- Jones, P.G.W., Folkard, A.R. 1971. Hydrographic observations in the eastern Irish Sea with particular reference to the distribution of nutrient salts. *Journal of the Marine Biological Association UK*, 51, 159-182.
- Luyten, P.J., Jones, J.E., Proctor, R., Tabor, A., Tett, P., Wild-Allen. K. 1999. COHERENS - A Coupled Hydrodynamical-Ecological Model for Regional and Shelf Seas : User Documentation. MUMM report, Management Unit of the Mathematical Models of the North Sea, 914pp.
- Maier-Reimer, E., Sündermann, J. 1982. On tracer methods in computational hydrodynamics. In: M. B. Abbott and J. A. Cunge (eds.). *Engineering applications of computational hydrodynamics*, Vol. 1. Pitman, Boston, London, Melbourne.
- Marsh, T.J., Sanderson, F.J. 2003. Derivation of daily outflows from Hydrometric Areas. Report prepared for the Proudman Oceanographic Laboratory, National River Flow Archive, CEH Wallingford, July 2003, 14 pp.
- Petersen, W., Petschatnikov, M., Schroeder, F., Colijn, F. 2003. Ferry-Box Systems for Monitoring Coastal Waters. in: Dahlin, H.; Flemming, N.C.; Nittis, K.; Petersson, S.E.: Building the European Capacity in Operational Oceanography, Proc. Third International Conference on EuroGOOS, Elsevier Oceanography Series Publication series 19, 325-333.
- Plüß 1999. Nordseemodell der BAW-AK, Berechnung der Tidedynamik in der Nordsee und der Deutschen Bucht, Report Bundesamt für Wasserbau, in German.
- Proctor, R., James, I.D. 1996. A fine-resolution 3D model of the southern North Sea. *Journal of Marine Systems*, 8, 285-295.
- Sharples, J., Simpson, J.H. 1995. Semi-diurnal and longer period stability cycles in the Liverpool Bay region of freshwater influence. *Continental Shelf Research*, 15 (2-3), 295-313.
- Wehde, H., Backhaus, J. O., Hegseth, E. N. 2001. The influence of oceanic convection on primary production, *Ecol Mod* 138, 115-126
- Wehde, H., Petersen, W., Petschatnikov, M., Schroeder, F., Colijn, F. 2003. Development and distribution of plankton observed with a Ferrybox system for monitoring coastal waters. ICES Annual Science Conference, September 24-27, 2003, Tallinn, Estonia.
- Young, E.F., Holt, J.T. 2005. Long-term variability of temperature and salinity in the Irish Sea. Submitted to *Journal of Geophysical Research*.

